NASA TECHNICAL NOTE

NASA TN D-3683

NASA TN D-3683

LIMITATIONS ON INERTIAL SENSOR TESTING PRODUCED BY TEST PLATFORM VIBRATIONS

by Herbert Weinstock

Electronics Research Center

Cambridge, Mass.

NATIONAL AERONAUTICS AND SPACE ADMINISTRATION • WASHINGTON, D. C. • NOVEMBER 1966

NASA TN D-3683

LIMITATIONS ON INERTIAL SENSOR TESTING PRODUCED BY TEST PLATFORM VIBRATIONS

By Herbert Weinstock

Electronics Research Center
Cambridge, Mass.

NATIONAL AERONAUTICS AND SPACE ADMINISTRATION

For sale by the Clearinghouse for Federal Scientific and Technical Information
Springfield, Virginia 22151 – Price $2.50

LIMITATIONS ON INERTIAL SENSOR TESTING PRODUCED BY TEST PLATFORM VIBRATIONS

By Herbert Weinstock
Electronics Research Center

SUMMARY

The calibration of precision inertial sensors is currently limited by drifts and oscillations of the position of the instrument's test platform relative to the axis of rotation of the Earth and the local gravity vector. For gyroscope testing, the analyses and measurements discussed in this document indicate that the most severe errors will result from angular motions of the platform at frequencies less than 100 cps. Under static conditions, a 1-arc second variation in platform position may result in an unwanted Earth rate component of 0. 075 millideg/hr. Current estimates of gyroscope performance in 1970 indicate drift rates of 0. 1 millideg/hr.

Measurements made in the vicinity of the NASA Electronics Research Center Guidance Laboratory in the Kendall Square area of Cambridge, Mass., indicate tilts of the order of 10 arc seconds with a 24-hour period from peak to peak. A 1-arc-second variation at a frequency of 1 cycle/min, which might correspond to local traffic and seismic activity, would result in an indicated rate of 0. 1 deg/hr (100 millideg/hr). For accelerometer testing, the errors in indicated performance are primarily caused by the component of gravity, caused, in turn, by rotations of the platform and vibratory accelerations. A rotation of 1 arc second represents a 5-micro-g acceleration error. Studies of vibration isolation techniques that will permit testing of inertial sensors in an urban location are being conducted at NASA's Guidance Laboratory.

This document reviews the limitations on instrument testing imposed by environmental conditions and briefly discusses the design studies being conducted to eliminate these limitations.

I. INTRODUCTION

The calibration of precision inertial sensors is currently believed to be limited by translational and angular vibrations and long-term tilts of the test platforms on which the instruments are calibrated. This has resulted in a search for seismically inactive locations for inertial sensor test facilities by instrument manufacturers and test laboratories. Some of these efforts were discussed in papers presented at the Symposium of the Test Pad Stability Subcommittee[1] of the American Institute of Aeronautics and Astronautics, held in Minneapolis, Minn., in August 1965. Most of these papers were concerned with measurements of long-term tilts and the magnitudes of the vibratory accelerations at a given test location. Of particular note was a description of the efforts of The Martin Company in obtaining a site for their test facility in a seismically inactive location near Denver, Colorado. In constructing the facility, however, they found that the cultural activity introduced by personnel and equipment necessary to the facility, combined with the resonances of the facility structures, resulted in acceleration levels above their stated tolerance. The papers[2,3] describe the considerable efforts of The Martin Company and their consultants in reducing the vibration levels. Although it may be possible to locate a sufficiently inactive test location someplace on the Earth and to take sufficient precautions in the design of the facility to permit testing of current instruments, the accuracy requirements of future instruments will require definition and control of the test environment to better accuracies than those permitted by the stability and seismic activity of known test locations. In addition, there are several situations where it is desirable to test the instruments at locations having known high seismic activities. For example, it is often necessary to calibrate an instrument at a space vehicle launch site. Also the location of a test facility is often influenced by considerations of the availability of skilled personnel and its proximity to established complementary test facilities. This Technical Memorandum reports progress on a study directed towards the design of an actively controlled vibration isolation system for a platform suitable for testing of inertial sensors.

The first problem in this design study was to establish the limits of the vibratory motions that were, in fact, tolerable in the testing of an inertial sensor. For the most part, the discussions of the Test Pad Stability Symposia did not relate the vibration measurements and tilt measurements reported to instrument test accuracies. In the presentations, a vibratory acceleration of several micro-g units was considered equally detrimental at all frequencies. This is not true. As discussed in Section II, for most applications, high-frequency accelerations will have a negligible effect on the indicated performance of the instrument. If the data from the instrument are averaged for a 10-second period, an acceleration of 100 micro-g at 1 cps would represent an error of 32 micro-g in indicated performance. The same acceleration at 50 cps (if the instrument had a flat frequency response) would produce an indicated error of 0.64 micro-g. In addition, the response of many acceleration sensors falls off with increasing frequency. A figure of merit that can be calculated from the measured tilts and translational and angular vibration frequency spectra is presented in Ref. 4 for single degree of freedom gyroscope instruments. Ref. 4, however, places undue emphasis on the steady-state vibration errors introduced by high-frequency vibrations of a magnitude which do not occur in practice. As discussed in Sections II and III, the largest errors (in practice) in gyroscope testing are caused by the rates associated with angular vibration of the test platform. The discussion of free-rotor gyroscope

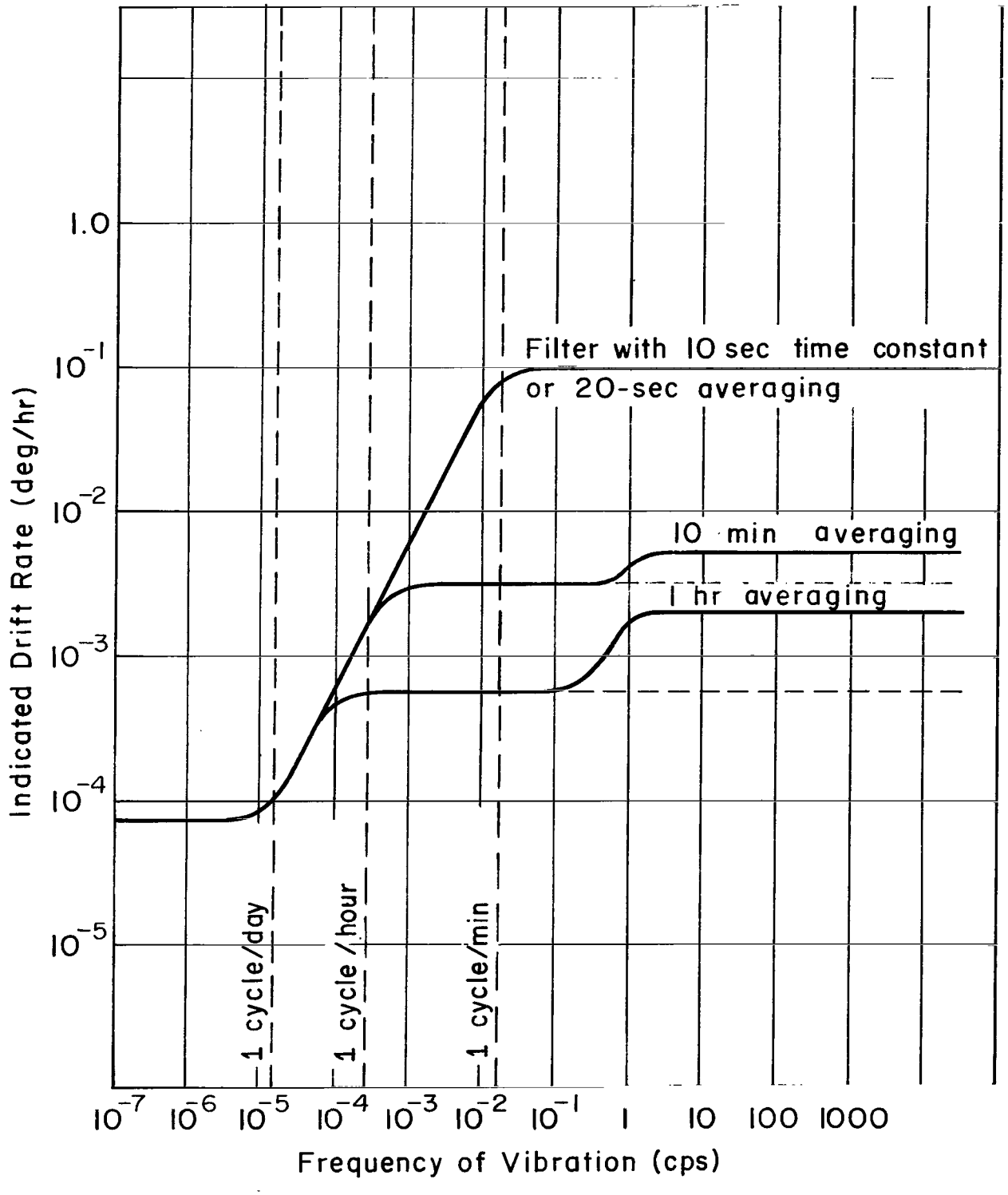

Figure 1.- Maximum error in gyroscope testing due to 1-arc second (vector) angular vibration versus frequency

testing by Wardin and Werner[5] considers only the long-term average error in testing introduced by long-term tilts. Accordingly, Section II reviews the relations between the motions and tilts and the resulting gyroscope and accelerometer test errors. Figure 1 shows the error that will result from a 1-arc second angular vibration in a gyroscope test as a function of the vibration frequency. Section II concludes that translational vibrations of the magnitude given in Section III (representing the test vibration environment) will have no effect on gyroscope testing to an accuracy of 0.01 millideg/hr.

However, for low-level accelerometer testing, the magnitude of specific force (combined effect of acceleration and gravity) and the frequency of vibration compared to the instrument response are critical and the effects of angular vibration are essentially negligible. Accordingly, the feasibility of two stabilized isolated platform designs are being considered:

1. A platform free from rotational motions producing indicated rates of 0.01 millideg/hr in a gyro test (not isolated from transitional vibrations)

2. A platform with horizontal plane free from translational accelerations of 0.1 micro-g (not isolated from rotational motions).

The reference for these angular motions will be defined by the average direction of the vertical over a 1-month period and the direction of the axis of rotation of the Earth. The reference for the translational motions will be a zero specific force (combined effect of acceleration and gravitational fields) in a plane of the platform.

An attempt at building a passively isolated platform to meet both the translational and rotational motion requirements by the Heath Air Force Station at Newark, Ohio, is reported in Ref. 6. A 24-foot, spring-supported pendulum (shown schematically in Figure 2) was constructed. The pendulum has natural frequencies of about 0.2 cps.

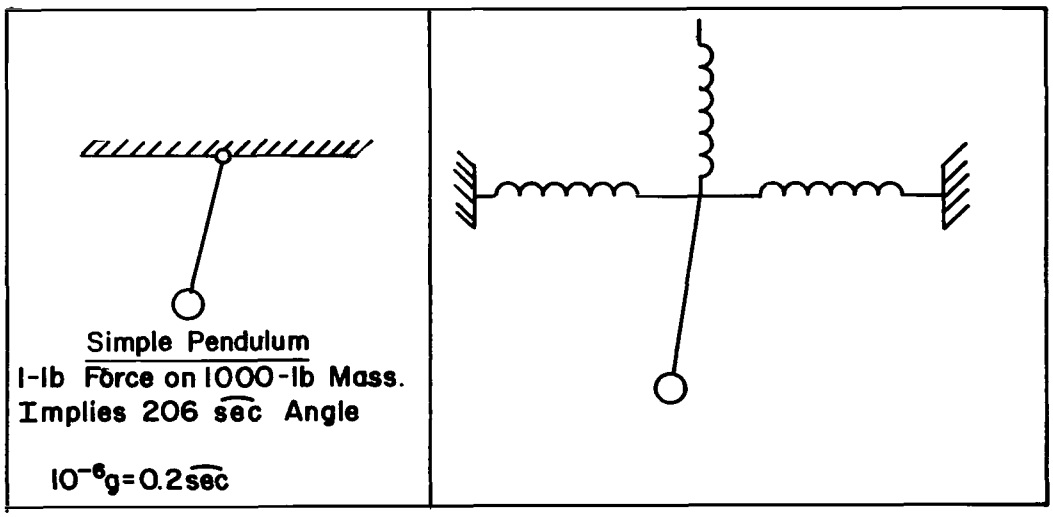

Figure 2.-Schematic of Heath pendulum -- High sensitivity to small disturbing forces

Although this system did provide vibration isolation at high frequencies, it was difficult to prevent undesirable oscillations at low frequencies because of small disturbance forces (e. g., convection currents). In addition, for any pendulum device, a force of 0. 001 of 1 percent of the weight of the pendulum is sufficient to produce an angular motion of 2 arc seconds. For a 200, 000-pound platform, a 2-pound force would be sufficient to produce a 2-arc-second displacement. In addition, if we assume an average density of the platform of about 500 lb/ft^3 (almost solid steel), the density of air being about 0. 075 lb/ft^3, a force equal to 10 percent of the weight of the air displaced by the platform would be sufficient to produce a 3-arc-second displacement.

A hypothetical zero-stiffness vibration isolation system would have an acceleration of 15 micro-g because of this force. To build a passive isolation system for testing inertial sensors would require building the platform with the same tolerances and environmental control (temperature, pressure, electromagnetic fields) required for precision inertial sensors. On the assumption that this could be done for a typical test turntable load of 2000 pounds, the platform would have to be totally enclosed and personnel could not be permitted in the test area.

Since instruments have been built which are capable of measuring accelerations of the order of micro-g accelerations and smaller (see e. g., Figure 3), a more practical means of providing low-frequency isolation is the use of an actively controlled servomechanism. Such a system, making use of an assembly of components designed and built for other projects, has been built at the MIT Instrumentation Laboratory.[7] A schematic diagram of this system is shown in Figure 4. A block diagram of the system (obtained from discussions with the designer) is shown in Figure 5. As shown by the root-locus plot of Figure 6, the bandpass of this system is limited by the time constant of the tilt transducer (a level vial) and the damping available in the system. In the existing system the network G (S) is not used for compensation. The time constant of the transducer is of the order of 10 seconds. The damping has not been measured. For purposes of this discussion, a ratio of effective moment of inertia to damping of 3 seconds is assumed. The response of this type of system to θ_0 is given by:

$$\frac{\Phi}{\theta_o} = \frac{1}{\left(1 + \frac{j\omega}{\omega_a}\right) \left[\left(1 - \frac{\omega^2}{\omega_n^2}\right) + 2\beta j \frac{\omega}{\omega_n}\right]} \tag{1}$$

where ω_a is the real root of the system characteristic equation shown in Figure 6. As shown by Figure 6, ω_a is considerably larger than ω_n. For purposes of approximation, it is therefore assumed that ω/ω_a is approximately zero for the frequency range of interest. The system becomes equivalent over the frequency range to a simple damped spring mass system:

$$\frac{\Phi}{\theta_o} = \frac{1}{\left(\left(1 - \frac{\omega^2}{\omega_n^2}\right) + 2\beta j \frac{\omega}{\omega_n}\right)} \tag{2}$$

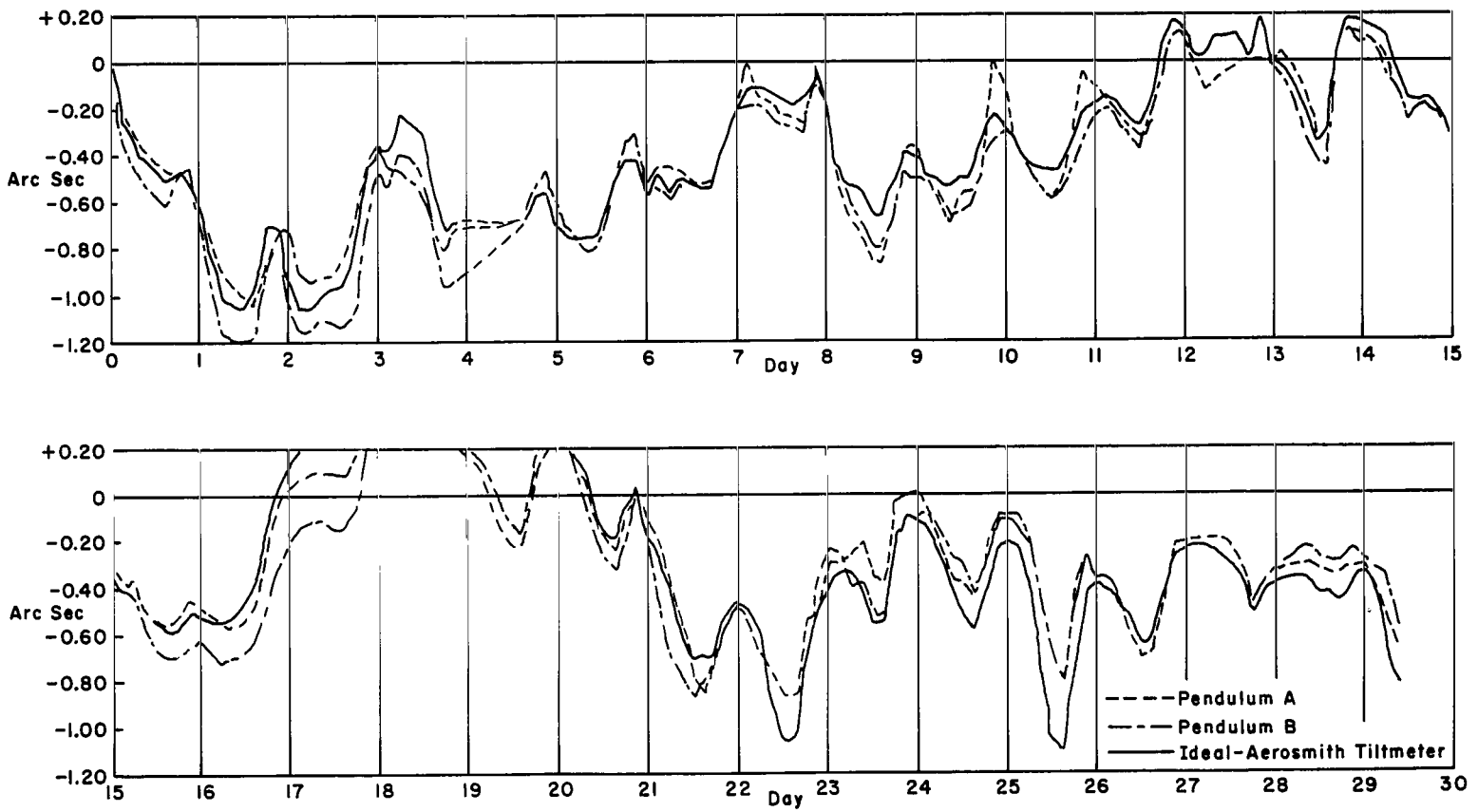

Figure 3.- Measurements made with three instruments at MIT Instrumentation Laboratory Facility, Bedford, Massachusetts (Ref. 10)

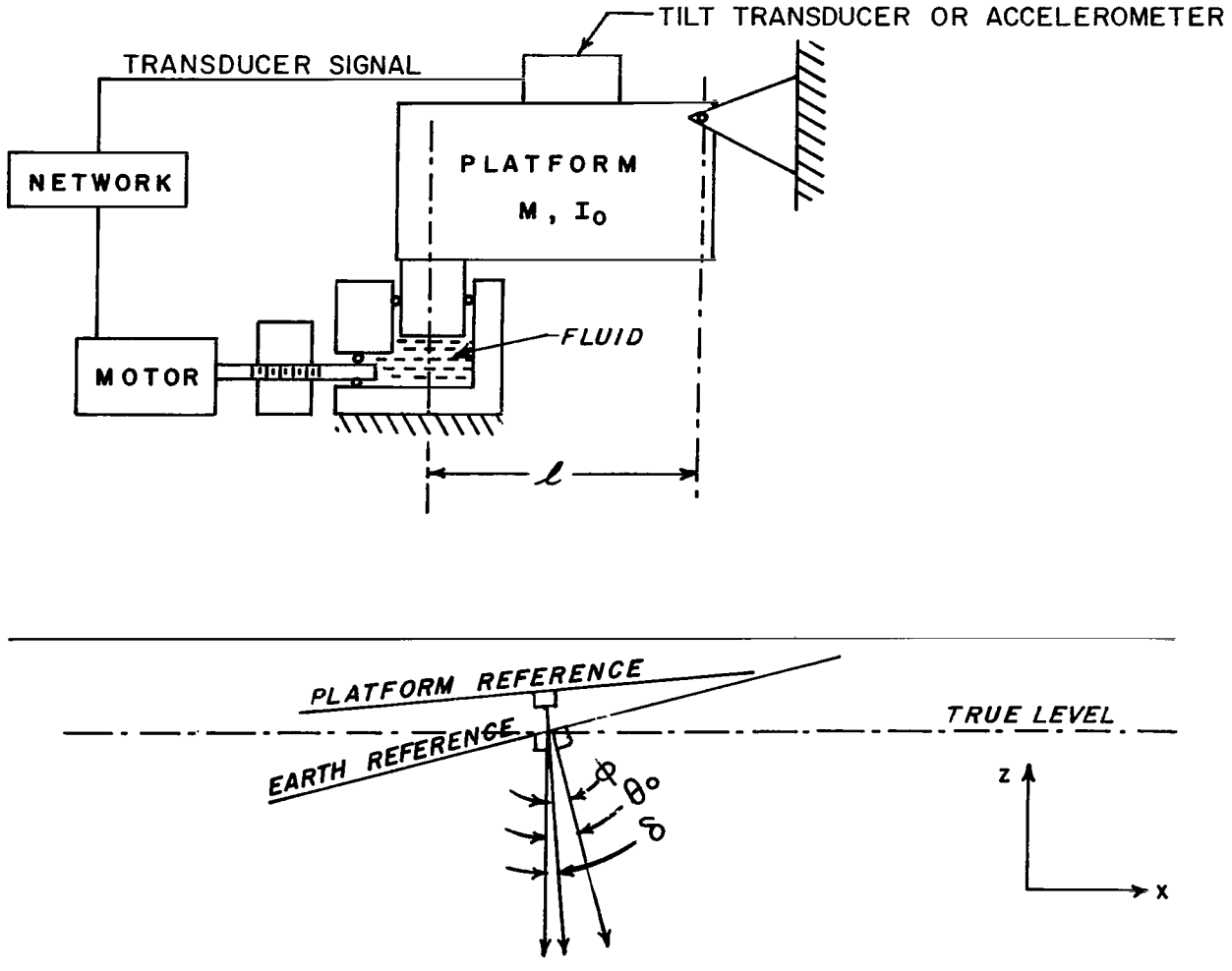

θ_o **Angle between Normal to Earth Surface and "True" Vertical.**

ϕ **Angle between Platform Normal and Earth Surface Normal.**

δ **Angle between Platform Normal and True Vertical.**

Figure 4.- Schematic of MIT Instrumentation Laboratory servo-controlled platform (top) and definition of coordinates for level of platform (bottom)

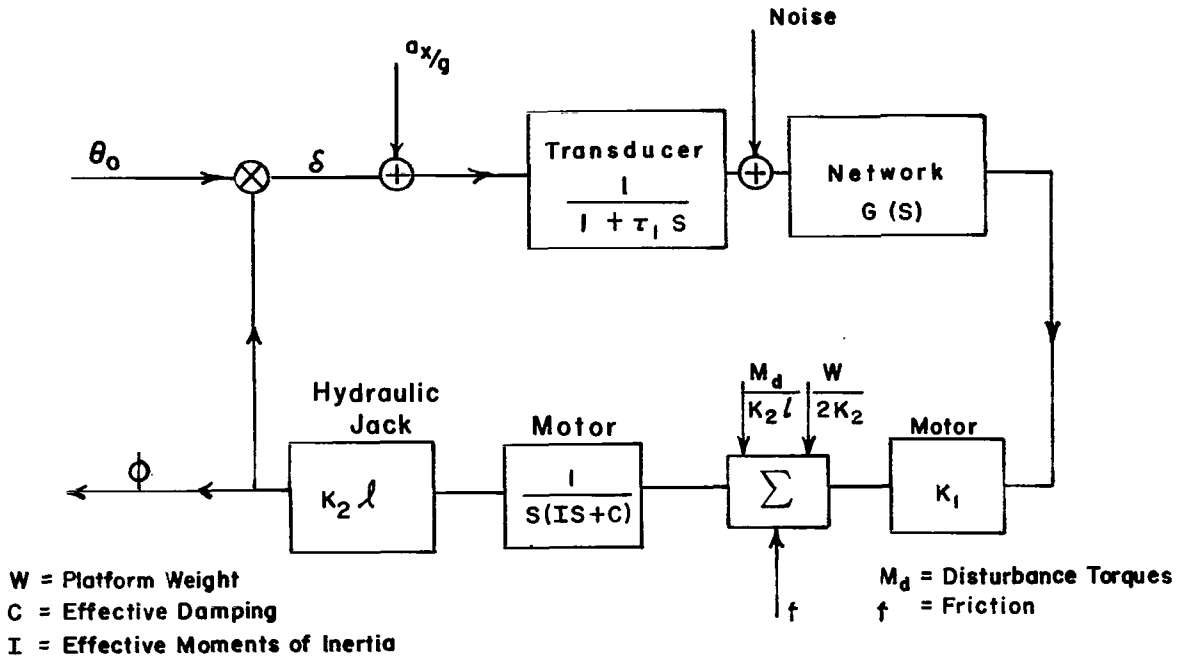

Figure 5.- Schematic of MIT Instrumentation Laboratory servo-controlled platform

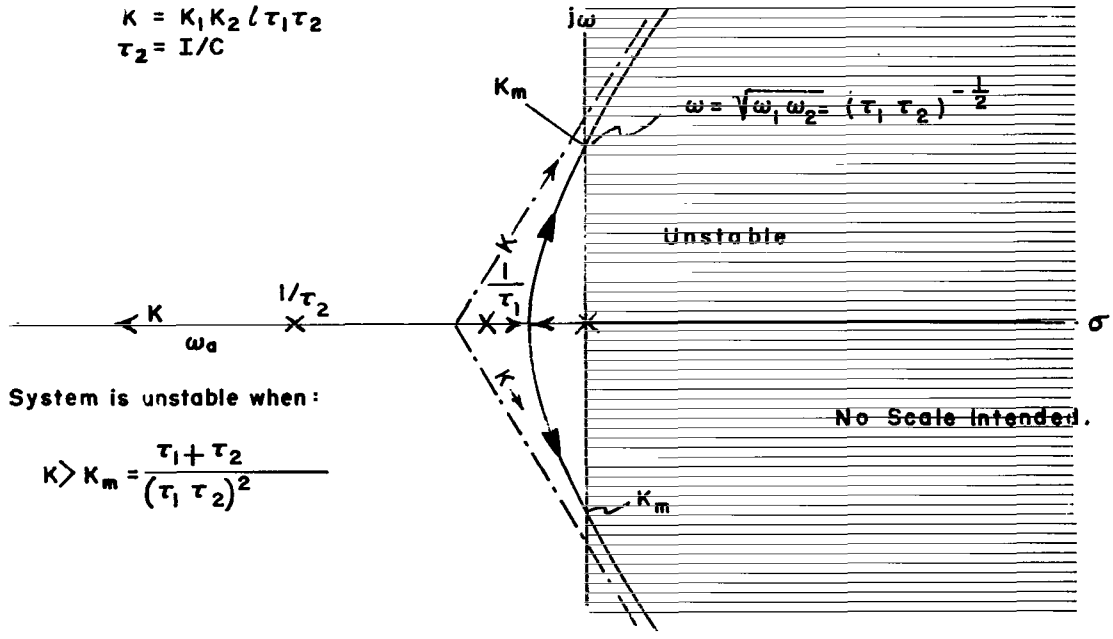

Figure 6.- Plot of root locus for MIT Instrumentation Laboratory servo-controlled platform

The error angle δ is thus:

$$\left|\frac{\delta}{\theta_o}\right| = \sqrt{\frac{\omega^2/\omega_n^2 \left(4\beta^2 + \omega^2/\omega_n^2\right)}{\left(1 - \frac{\omega^2}{\omega_n^2}\right)^2 + 4\beta^2 \frac{\omega^2}{\omega_n^2}}} \qquad (3)$$

For frequencies near and above the natural frequency, the system produces errors in the angular position relative to true vertical that are larger than the Earth motions (θ_o). With the time constants given above, the maximum possible natural frequency is 0.18 rad/sec or about 0.03 cps which is 1.8 cycle/min. Based on Figure 6, this implies an actual natural frequency of about 0.6 cycle/min for adequate damping.

In construction of this platform, the designers did note the instability with increased gain discussed above. Measurements made on the performance of this system by NASA-ERC personnel using an electronic pendulous level with a natural frequency near 5 cps indicated no deviation of the platform from the vertical over long periods to within ±1 arc second. This performance was achieved in the presence of long-term tilts of the order of 10 arc seconds (see Figure 7). However, over short periods and for high frequencies the system appears to act as an amplifier. Figure 8 shows the transient effect caused by a man approaching the platform to mark the time of a reading. The indicated platform excursion is 2.5 times the motion of the base. The performance of the system can be improved through the use of a transducer with a faster response, with velocity and possibly position feedback to the motor (K_1), and by compensation networks. However, the level vial or an accelerometer cannot distinguish between rotations relative to the vertical and horizontal accelerations. An estimate of the power spectral density of the accelerations of a test station in a busy urban location, as obtained in Section III, is shown in Figure 9. If the system bandpass were extended to 10 cps, the system would see accelerations of at least 1 micro-g and possibly up to 0.001 g. This maximum acceleration would result in an intolerable motion of the order of 200 arc seconds. The smallest motion of 0.2 arc second would exceed our design limit.

Under Contract NAS 12-74 with NASA's Electronics Research Center, the Northrop Nortronics Division of Norwood, Massachusetts, has conducted a study of the feasibility of using gyroscope instruments for control of an active angular vibration-isolation system. The initial premise of this study was that Earth-bound system sensor requirements would always be more severe than aeronautical and/or astronautical mission requirements. However, assuming a gyroscope drift rate of 0.1 millideg/hr, there would be an undesired Earth-rate component of 0.1 millideg/hr at the end of 4 hours or a platform drift of 9 arc seconds/day. To control the low-frequency drift of the platform, accelerometers were added to the control loops. A schematic drawing of the system proposed by Nortronics in their final report is shown in Figure 10.

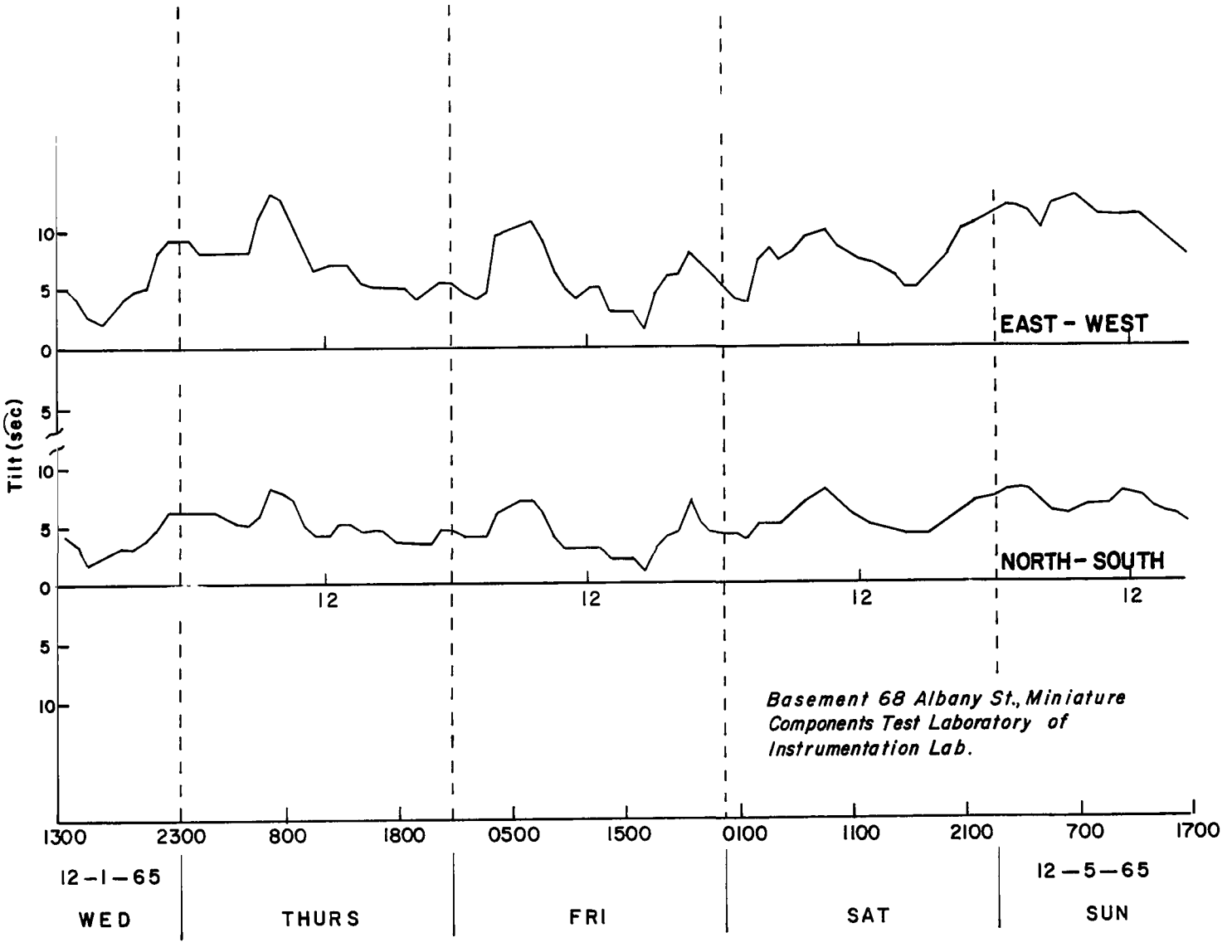

Figure 7.- Tilt measured on concrete base in miniature components test (FBM) area of MIT Instrumentation Laboratory basement, 68 Albany Street, Cambridge, Mass.

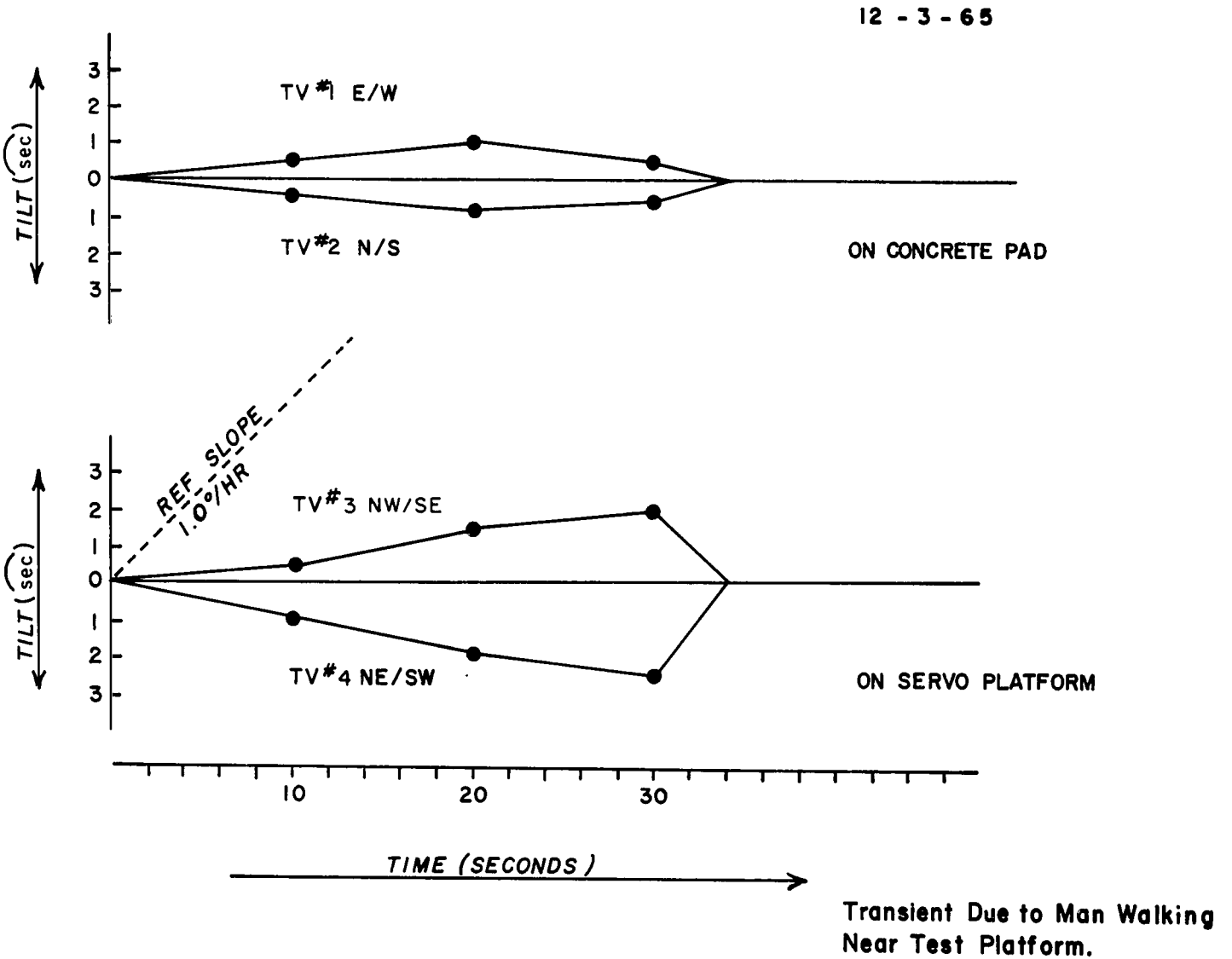

Figure 8.- Transient tilt of servo-levelled test platform in miniature components (FBM) test area of MIT

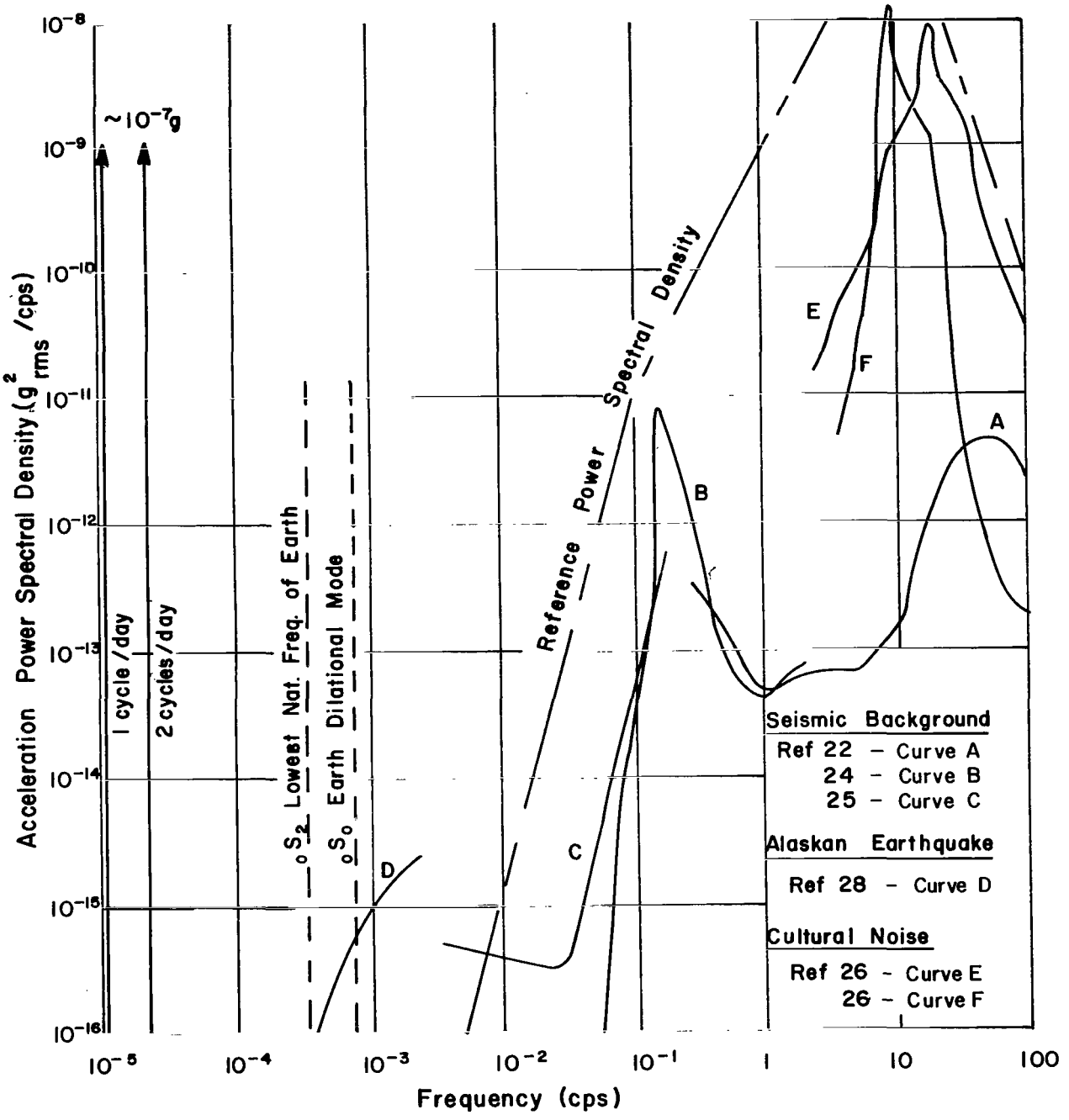

Figure 9.- Representative acceleration power spectral density for test station

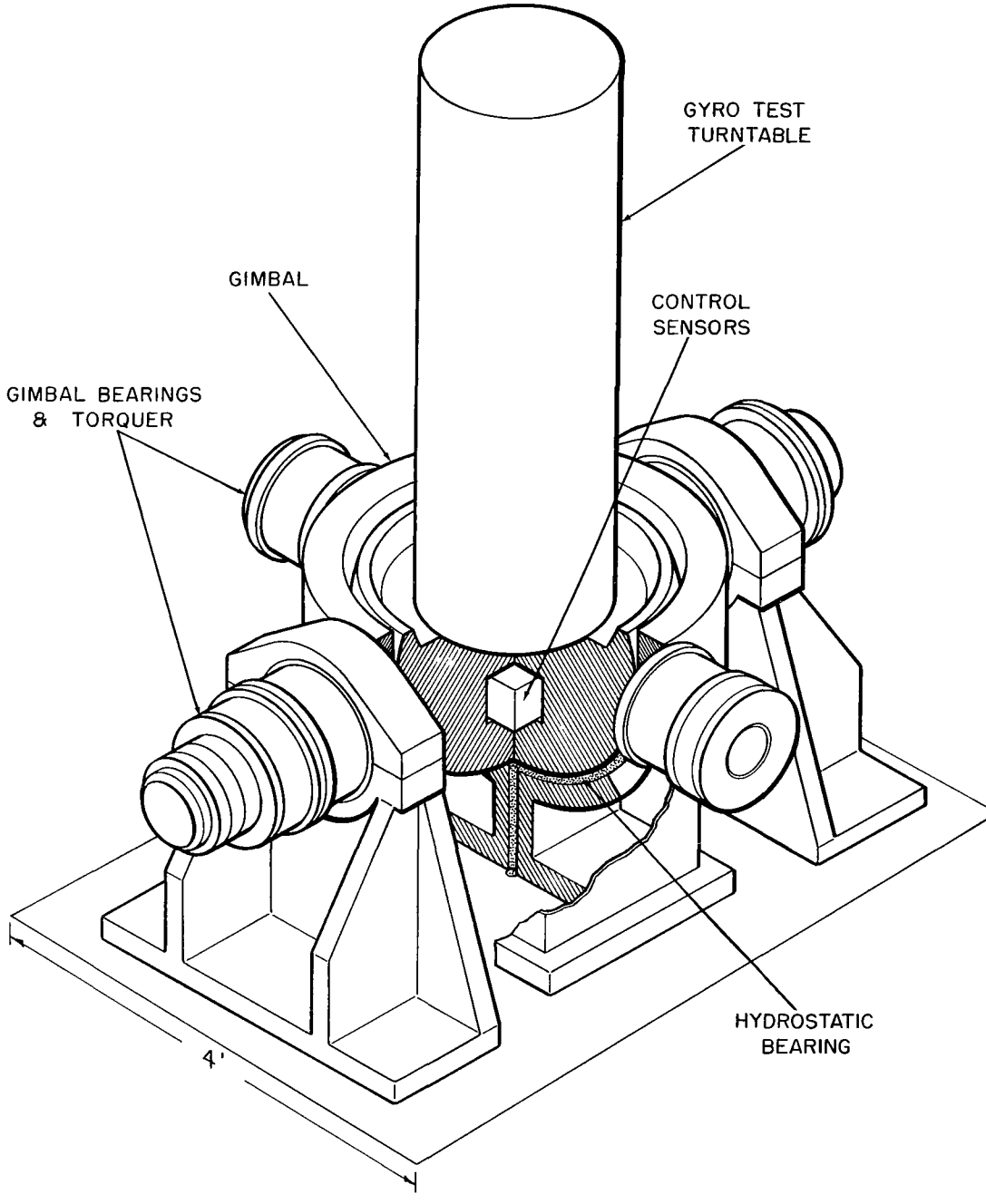

Figure 10.- Schematic of Nortronics-proposed isolation system (from Nortronics final report, contract NAS 12-74, 3/25/66)

They proposed that the test platform be hydrostatically supported on a spherical bearing and torqued through two gimbals. A block diagram of the control loop proposed is shown in Figure 11. At low frequencies, the platform is to be controlled by the accelerometer and at higher frequencies the gyroscope instrument is to assume control. The "transition" frequency was calculated at 0.0015 cps based on the smallest accelerometer gain that could be used to compensate for a low-frequency gyroscope drift of 0.1 millideg/hr and a control error of 0.01 arc second. Since gyroscope drift rate is known to vary essentially as a random walk at low frequencies (see e.g., Refs. 8 and 9) an integrating loop is used to compensate for the long-term gyro drift rate. Since the gyroscope used in the analysis has a relatively long time constant (about 0.7 second), strong lead compensation has been used to extend the bandpass of the servo system to a calculated 1350 cps. The analysis unfortunately does not consider the effects of high-frequency components on gyroscope drift rate and has not included a complete consideration of the instrument error models. As shown in Figure 12, gyroscope instruments do have sizable drift rate components at higher frequencies where the noise generated by the rotating wheel and electrical torques begin to become significant. It should be noted that the data of Figure 12 has been effectively filtered by a measurement scheme having approximately a 4-cps bandpass. It is contended that a significant portion of this high-frequency rate is caused by angular motion of the base of the test platform; however, no measurements have been made to confirm this contention on the instrument being considered. The Nortronics analysis does not optimize the system with respect to the frequency spectra of the environment and instrument errors. The use of gyroscopes other than those having the approximate characteristics of one of the Nortronics SINS gyro has not been considered. The possibility of passive inertia isolation at high frequencies is not considered.

Another scheme for distinguishing between rotational and translational motions is the use of a simple damped pendulum as shown schematically in Figure 13. At very low frequencies, a pendulum is held to the vertical by the restraint of gravity. At high frequencies, inertia tends to keep the pendulum at rest with a signal output proportional to the rotational displacement of the case. At high frequencies, this inertia also makes the pendulum insensitive to acceleration. At intermediate frequencies, however, the pendulum is very sensitive to acceleration and insensitive to rotation. If the disturbances are small at these frequencies, the system can conceivably be effective.

The proper design of any of the above systems demands a knowledge of the acceleration and rotation environment in which the system operates. Section III reviews the results of efforts to describe these environments and presents the measurements obtained to date.

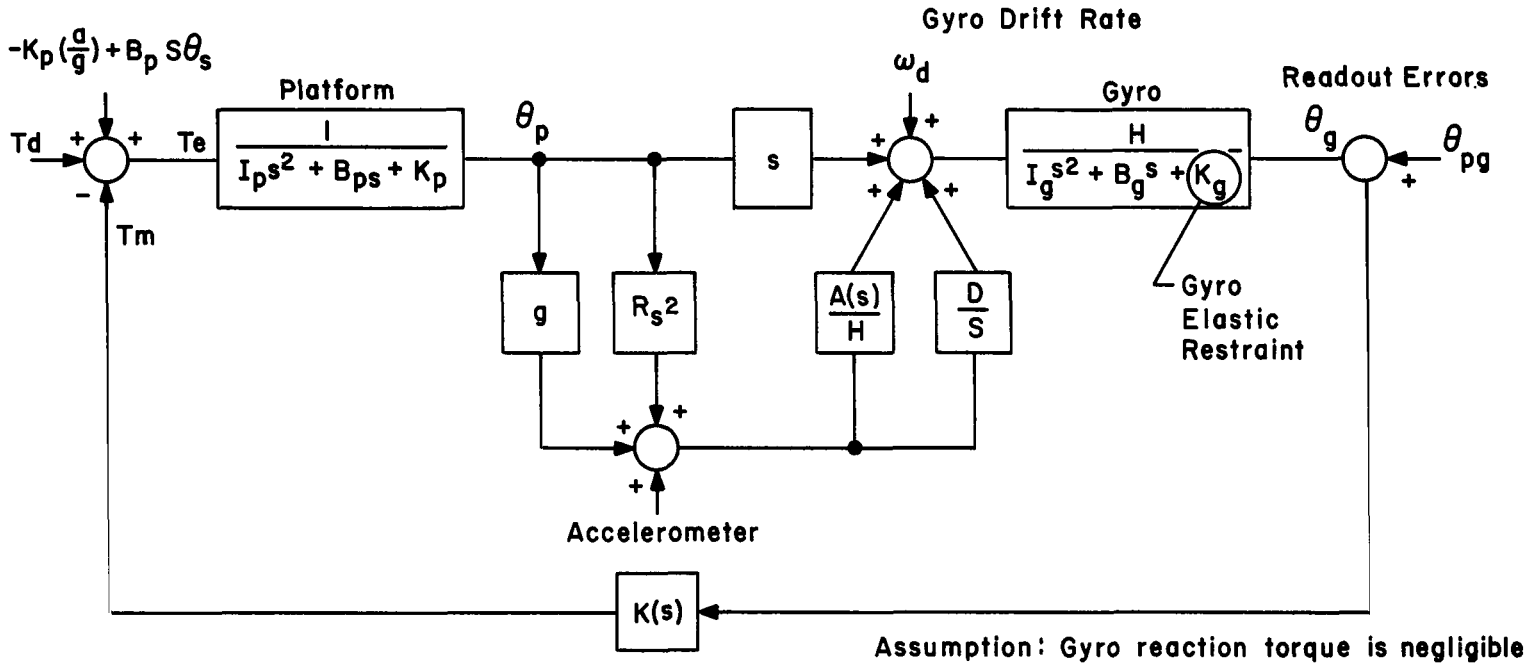

Figure 11.- Block diagram of pad controlled by gyro and accelerometer (from Nortronics final report, contract NAS 12-74, 3/25/66)

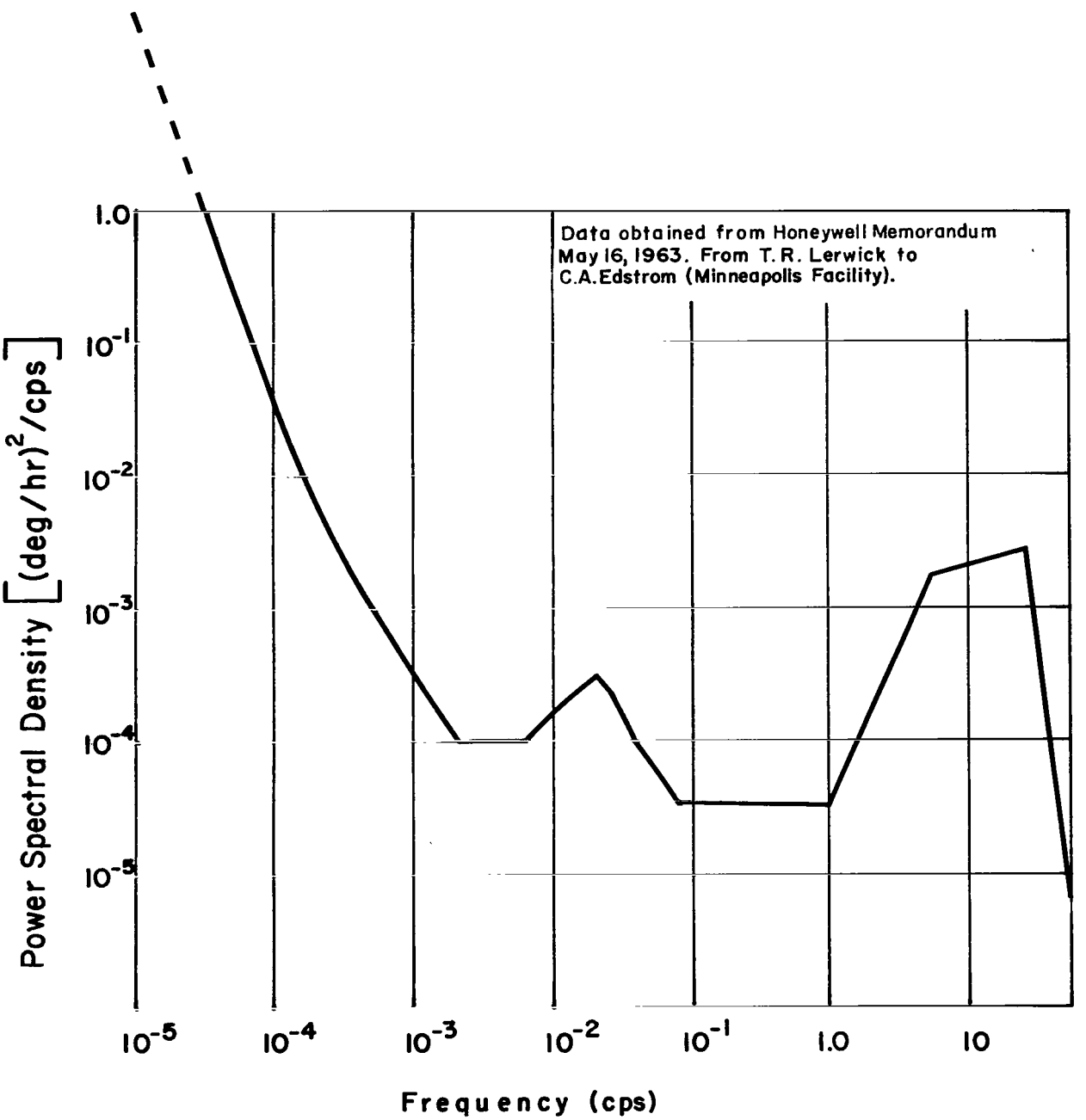

Figure 12.- Estimated power spectral density of gyroscope drift rate--Honeywell gyro model No. CG159 C1, Unit No. 5

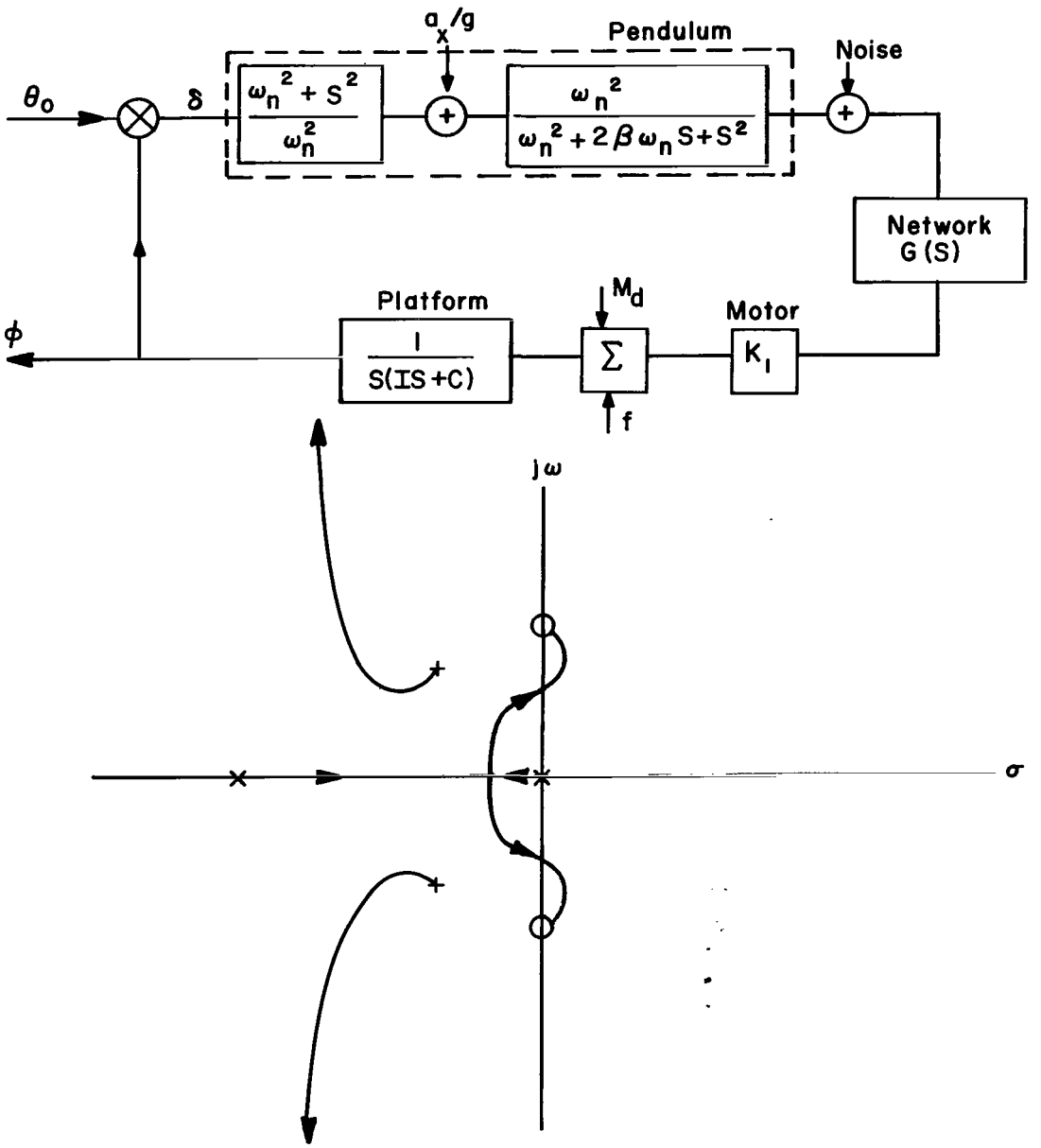

Figure 13.- Block diagram of pendulum-controlled system using drive of figure 4 (top) and root locus of pendulum controlled system with no compensation (bottom)

II. PERMISSIBLE MOTIONS OF THE TEST PLATFORM

Introduction

To test a precision instrument, it is essential that the environment in which the instrument is tested does not introduce inputs to the instrument, the combined effect of which is not defined to an accuracy of one order of magnitude greater than the accuracy desired of the instrument under test. If a gyroscope or accelerometer is tested on a platform which is not perfectly stationary with respect to its Earth-reference coordinate system, there will be inaccuracies in the test results. These inaccuracies will be caused by the following factors:

1. Uncertainties in the orientation of the instrument relative to the angular velocity of the Earth and to the direction of gravity
2. Angular vibrations of the test platform
3. Translational vibrations of the platform.

The magnitude of the maximum possible errors in gyroscope and accelerometer testing which can be expected for each of the above factors is estimated in the following paragraphs. For reference purposes, these factors are used to specify the allowable motions of inertial sensor test platforms for testing gyroscopes having drift rates of 0.1 millideg/hr, and for testing accelerometers to an accuracy of 0.000001 of gravity (1 micro-g).

Errors Due to Uncertainty in Orientation of the Instrument

If a gyroscope is mounted with its sensitive axis at an angle of θ to the axis of rotation of the Earth, the gyroscope will sense a component of the angular velocity of the Earth of:

$$\omega_{IA} = \omega_{(I-E)} \cos \theta \tag{4}$$

where

ω_{IA} = angular velocity about the gyroscope-sensitive axis

ω_{I-E} = angular velocity of the Earth relative to inertial space

θ = angle between the gyroscope-sensitive axis and the Earth's polar axis.

If the angle θ is in error by a small angle ϵ'_o, the gyroscope will sense a rate of:

$$\omega_{IA} = \omega_{I-E} \cos (\theta \pm \epsilon'_o) \approx \omega_{IE} (\cos \theta \mp \epsilon'_o \sin \theta). \tag{5}$$

Since the angular velocity of the Earth is 15 deg/hr, the error in the measured rate is:

$$E = 15\,\epsilon_o'\,\sin\theta \tag{6}$$

where E is the error in rate (deg/hr) and ϵ_o' is the misalignment angle (radians). This error is a maximum when the gyroscope is oriented with its sensitive axis perpendicular to the Earth axis. This is a fairly common test mode for obtaining the acceleration sensitivities of both single degree-of-freedom and 2 degree-of-freedom gyroscope instruments. The maximum gyroscope test error due to uncertainity in orientation relative to Earth axis is:

$$E_{max} = 15\,\epsilon_o' = 0.000073\,\epsilon_o \tag{7}$$

where ϵ_o is the misalignment angle (seconds of arc).

A drift of a test platform of 0.2 second of arc would thus result in a test error of 0.000015 deg/hr.

Similarly, if an accelerometer test had an uncertainty in orientation relative to the gravity vector of 0.2 arc second, the maximum error due to this uncertainty would be 1 micro-g.

For a gyroscope instrument, the error of the indicated rate caused by a 1 gravity acceleration is generally small compared to Earth rate. The error due to misalignment of the instrument relative to gravity is of the order of ϵ_o' times the acceleration sensitivity and is thus negligibly small compared to the errors caused by misalignment with the polar axis. Similarly the errors caused by an accelerometer being misaligned with the angular velocity vector of the Earth are negligibly small compared to misalignments with the gravity vector.

Gyroscope Test Errors Due to Angular Oscillations

Since the gyroscope is a rate-sensing device, it will measure angular oscillations of the test platform about the input axis of the instrument. For an angular vibration displacement given by

$$A = a \sin \omega t.$$

There is an angular velocity of

$$\dot{A} = a\,\omega \cos \omega t.$$

The gyroscope will therefore sense a maximum rate for an angular vibration of amplitude a of

$$A_{max} = (2\pi f) \tag{8}$$

Thus for a 1-arc-second angular oscillation at 0.1 cps, the instrument will sense a rate of 0.628 arc sec/sec or 0.628 deg/hr.

In testing an inertial sensor it is common practice either to pass the data through a filter or to average the data for a period of time which is presumed to be long compared to disturbance inputs to the instrument. If the filter has the characteristics of a first-order system,

$$\frac{X_{out}}{X_{in}} = \frac{1}{1 + \tau s}$$

where

τ = filter time constant (sec) and

s = Laplace transform variable,

the indicated gyro rate is:

$$|\dot{A}| = \frac{|A| \; 2\pi f}{\sqrt{1 + (2\pi f)^2 \tau^2}} \tag{9}$$

where

f = frequency of angular vibration (cps)

τ = filter time constant (sec)

$|A|$ = magnitude of angular displacement (sec)

$|\dot{A}|$ = amplitude of rate indicated by measuring system about gyroscope input axis (deg/hr).

The indicated error in drift rate due to angular vibration is plotted for various filter time constants as a function of vibration frequency in Figure 14 for this mode of testing.

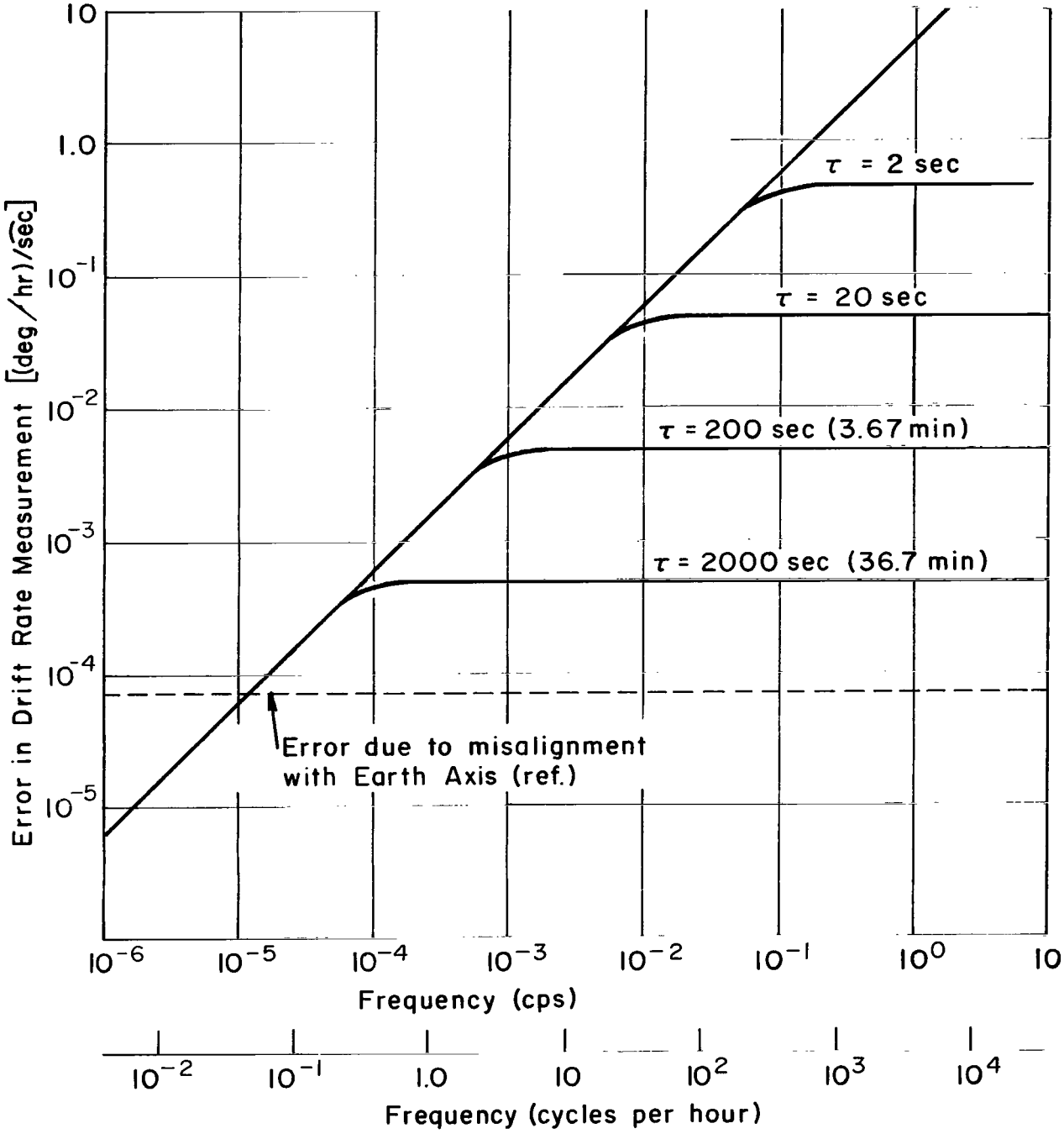

Figure 14.- Error in measured drift rate due to angular vibration about sensitive gyroscope axis versus frequency of vibration--Drift rate is assumed to be filtered by first-order filter with time constant of τ

If the drift rate is obtained by averaging the data for a period of time T, the indicated drift rate is simply the difference between the angular displacements at the beginning and end of the averaging period divided by the averaging time:

$$\dot{A}_{ind} = \frac{a \sin \omega(t_1 + T) - a \sin \omega t_1}{T} .$$

If the averaging time is long compared to the period of vibration and does not coincide with a multiple of the vibration period, the maximum indicated rate is:

$$\dot{A}_{I\,max} = \frac{2a}{T} . \tag{10}$$

The root mean squared indicated drift rate is:

$$\dot{A}_{I\,rms} = \frac{a\sqrt{(1 - \cos \omega T)}}{T} . \tag{11}$$

If there is a 1-arc-second angular oscillation and the averaging time is 10 minutes, the maximum indicated drift rate is 0.0032 deg/hr. The rms indicated drift rate is 0.0023 deg/hr. The effect of averaging time on the indicated gyro drift rate due to angular oscillations is illustrated in Figure 15. Appropriate averaging times for gyro drift rate measurements have been a long-standing issue of contention among gyroscope designers and manufacturers. The result of this disagreement has been a multiplicity of gyroscope test procedures, filter time constants, and corresponding instrument figures of merit.

Two instruments of different design may have the same quoted rms drift rates and an order of magnitude difference in actual performance, depending on the filtering used in processing the data. In tumbling tests* for a single-degree-of-freedom gyroscope, a common filter time constant is 25 seconds. In the inertial reference drift test (servo test), the typical averaging time is 40 minutes per data point. The tumbling test time constant is chosen arbitrarily to produce a compromise between the speed of testing and a "smooth trace" on the chart recorder used in the test. One of the reasons for the 25-second time constant is stray angular motion of the test platform. The averaging time of 40 minutes in the inertial reference drift test is intended to permit the test platform to rotate through a sufficiently large angle (10 degrees) to permit accurate drift angle measurements. Another advantage of the long averaging time is that a 10-degree data-taking interval requires processing of only 36 data points per turntable revolution while a 1-degree interval would require processing 360 data points. The development of automatic data handling and processing equipment over the past decade tends to minimize the importance of the latter advantage of longer averaging times.

*A description of typical gyroscope test procedures may be found in Refs. 12, 13, and 14.

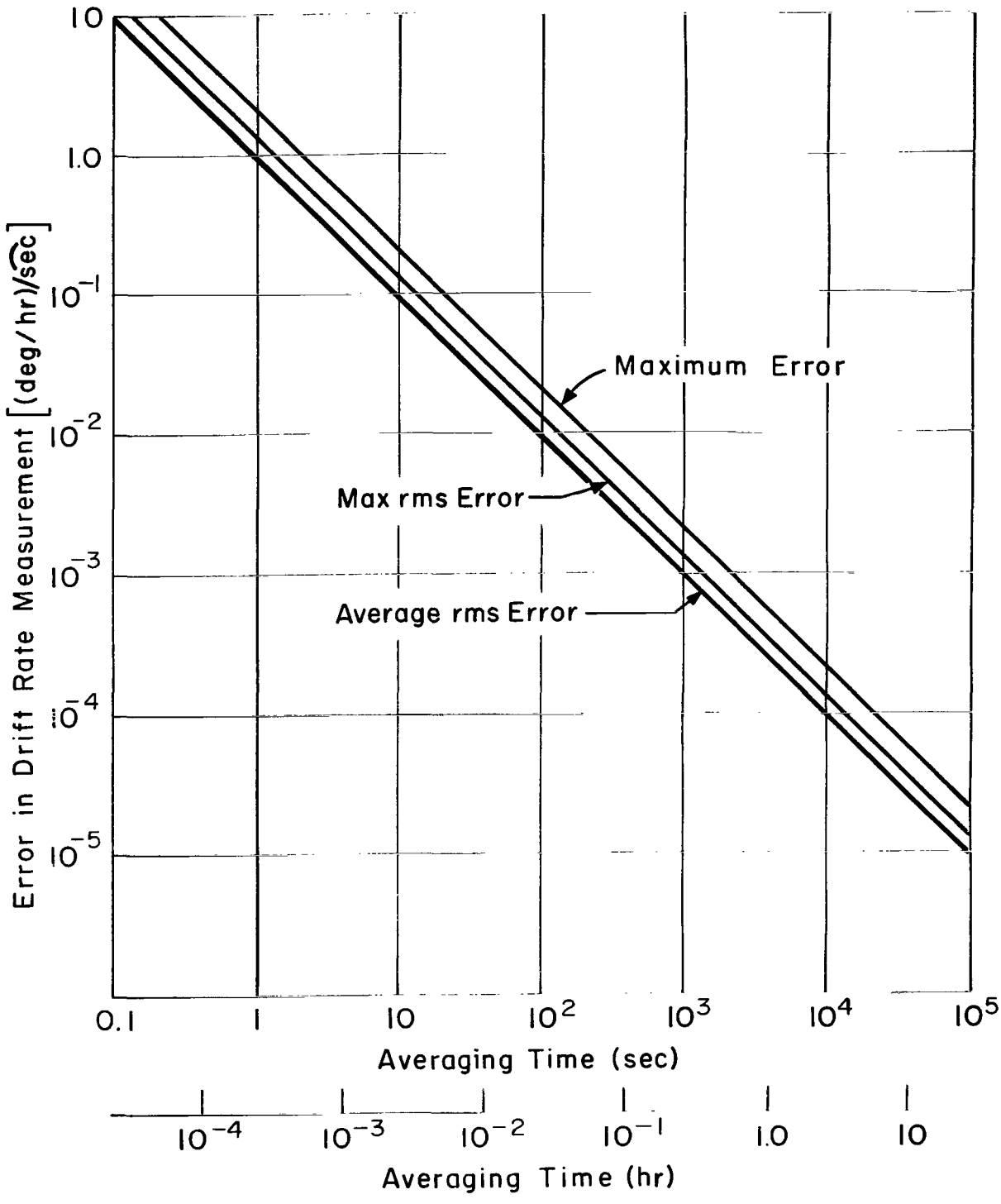

Figure 15.- Error in measured drift rate due to angular vibration about sensitive gyroscope axis versus averaging time--Drift rate is filtered by averaging over time period which is long compared to the period of the vibration

A stronger argument for the use of long averaging times is that in most applications an inertial quality gyroscope is used as an angular orientation transducer. Therefore, the final measure of gyroscope performance in application is the integral of gyroscope drift rate or drift angle. The measure of the averaging or filtering that may be permitted in a gyro test would be the speed and accuracy required in vehicle maneuvers in a given application. However, the time required for an instrument calibration is directly proportional to this averaging time. In addition, high-frequency noise signals may produce saturation or other undesirable effects in system use. In any event, the information about the gyroscope drift rate obtained in most gyroscope test procedures is strongly limited by the filtering and averaging employed in the test. For reference purposes it is assumed that the smallest filter time constant will be 10 seconds and the shortest averaging time will be 20 seconds. This implies that an angular motion of 0.001 arc second at frequencies greater than 0.1 cps will result in an indicated drift rate of about 0.0001 deg/hr.

In addition to the errors in the test results which are caused by the instrument measuring the instantaneous rate associated with the angular vibration, there is a steady-state error produced by angular vibrations that will exist in any rate or rate-integrating gyroscope. Since this angular vibration error has a steady-state component, it cannot be eliminated through the use of long averaging times. If a single degree-of-freedom rate-integrating gyroscope is subjected to angular vibrations about its spin and output axes, as shown schematically in Figure 16:

$$A_{SRA^*} = a \sin \omega t$$

$$A_{(I-C)OA} = b \sin \omega t + e \cos \omega t, \tag{12}$$

there is a rate about the instrument's reference input axis of:

$$\omega_{IRA} = A_{(I-C)OA} \dot{A}^*_{SRA}$$

$$= \frac{ab\omega}{2} \sin 2\omega t + \frac{ae\omega}{2} \cos 2\omega t + \frac{ae\omega}{2} \tag{13}$$

The average rate

$$\omega^*_{IRA} = \frac{ae\omega}{2} \tag{14}$$

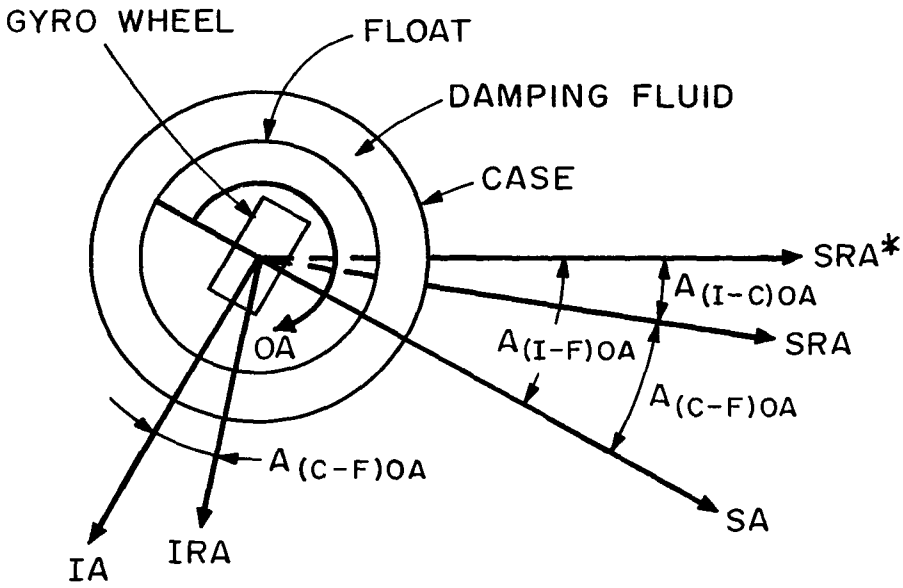

PERFORMANCE EQUATION :

$$C_d \dot{A}_{(C-F)OA} + (I_{FOA} + I_W)\ddot{A}_{(I-F)OA} = H\dot{A}_{IA}$$

DEFINING ; $\tau_o = \dfrac{(I_{FOA} + I_W)}{C_d}$ GYROSCOPE TIME CONSTANT;

$h = \dfrac{H}{C_d}$ GYROSCOPE GAIN

AND SINCE : $A_{(I-F)\,OA} = A_{(I-C)OA} + A_{(C-F)OA}$

WE HAVE : $\dot{A}_{(I-F)OA} + \tau_o \ddot{A}_{(I-F)OA} = h\dot{A}_{IA} + \dot{A}_{(I-C)OA}$

Figure 16.- Schematic of single-degree-of-freedom rate-integrating gyroscope

is the "coning" or "kinematic rectification" error described in Refs. 15 and 16. Since the gyroscope instrument is sensitive to the rate about the input axis of the gyroscope, the actual rate that will be sensed by the instrument is:

$$\omega_{IA} = A_{(I-F)OA}\, \dot{A}_{SRA^*} \quad . \tag{15}$$

Assuming the small angle approximations and a first-order system response,* the motion of the gyroscope float caused by the angular vibration about the instrument's output axis is:

$$A_{(I-F)OA} = \frac{A_{(I-C)OA}}{1 + j\tau\omega} = \frac{(b - e\tau\omega)\sin\omega t}{1 + \tau^2\omega^2} + \frac{(e - b\tau\omega)\cos\omega t}{1 + \tau^2\omega^2} \tag{16}$$

where

τ = gyroscope characteristic time

$j\omega$ = complex frequency variable

$j = \sqrt{-1}$.

The rate about the input axis is thus:

$$\omega_{IA} = \frac{a\omega(b - e\tau\omega)\sin 2\omega t + a\omega(e - b\tau\omega)\cos 2\omega t}{2(1 + \tau^2\omega^2)} + \frac{a\omega(e - b\tau\omega)}{2(1 + \tau^2\omega^2)} \quad . \tag{17}$$

The average rate due to angular vibrations about the spin and output axes is:

$$\omega^*_{IA} = \frac{a\omega(e - b\tau\omega)}{2(1 + \tau^2\omega^2)} \quad . \tag{18}$$

*The first-order approximation is strictly valid only for an infinitely stiff gyroscope float. It is, however, a good approximation for the range of frequencies of interest to this study. The effects of compliance on the frequency response of a gyroscope instrument is discussed in Ref. 17. The effects of compliance on the angular vibration errors is considered in Ref. 18.

Similarly, if there is an angular vibration about the gyroscope input axis of:

$$A_{(I-C)IA} = c \sin \omega t + f \cos \omega t , \tag{19}$$

the float response is:

$$A_{(I-F)OA} = \frac{h A_{(I-C)IA}}{1 + j\tau\omega} = \frac{h (c - f\tau\omega) \sin \omega t}{1 + \tau^2 \omega^2} + \frac{h (f - e\tau\omega) \cos \omega t}{1 + \tau^2 \omega^2} . \tag{20}$$

The drift rate due to the angular vibrations:

$$\left.\begin{aligned} A_{(I-C)SRA^*} &= a \sin \omega t + d \cos \omega t \\ A_{(I-C)OA} &= b \sin \omega t + e \cos \omega t \\ A_{(I-C)IA} &= c \sin \omega t + f \cos \omega t \end{aligned}\right\} \tag{21}$$

is therefore:

$$\omega^*_{IA} = \frac{\left[a (e + fh) - d (b + ch)\right] \omega}{2 (1 + \tau^2 \omega^2)} - \frac{\tau \left[a (b + ch) + d (e + fh)\right] \omega^2}{2 (1 + \tau^2 \omega^2)} . \tag{22}$$

The angular vibration represented above is the most general single-frequency angular vibration that may be applied to the instrument. The orientation of the unit with respect to the angular vibrations varies from one test orientation to another, changing the effective components of vibration about each of the unit axes. It is therefore useful to consider the effects of a coordinate transformation where the unit has been rotated with respect to a set of reference axes. The vibration components given above can be considered, in the manner of Ref. 4, as the components of two angular vibration vectors:

$$\begin{aligned} V_1 &= (\vec{i}a + \vec{j}b + \vec{k}c) \sin \omega t \\ V_2 &= (\vec{i}d + \vec{j}e + \vec{k}f) \cos \omega t . \end{aligned} \tag{23}$$

The squared magnitude of these vectors is given by

$$\epsilon_1^2 = a^2 + b^2 + c^2$$

$$\epsilon_2^2 = d^2 + e^2 + f^2 , \tag{24}$$

and they are separated by an angle given by

$$\sin\theta = \left| \frac{\vec{V}_1 \times \vec{V}_2}{|\vec{V}_1| \; |\vec{V}_2|} \right| . \tag{25}$$

We also have

$$\sin\theta = \left| (\vec{i}\ell_1 + \vec{j}m_1 + \vec{k}n_1) \times (\vec{i}\ell_2 + \vec{j}m_2 + \vec{k}n_2) \right|$$

where ℓ, m, and n are the direction cosines of the vibration vectors referred to the unit axes in a given orientation. In terms of the vector magnitudes and the direction cosines, the error is given by

$$E = \frac{\epsilon_1 \epsilon_2 \left[\ell_1 (m_2 + hn_2) - \ell_2 (m_1 + hn_1)\right] \omega}{2 (1 + \tau^2 \omega^2)}$$

$$- \frac{\tau \left[\epsilon_1^2 \ell_1 (m_1 + hn_1) + \epsilon_2^2 \ell_2 (m_2 + hn_2)\right] \omega^2}{2 (1 + \tau^2 \omega^2)} . \tag{26}$$

If the magnitudes of ϵ_1 and ϵ_2 were known and the angle between the two vectors were known, we could now proceed to find the direction cosines that would produce the maximum error. Unfortunately, if more than one frequency component is present in the vibration, it is difficult to measure the phase of the vibration components, and only the total squared magnitude of the vibration can be measured. This total vibration at a given frequency is defined as

$$\epsilon^2 = \epsilon_1^2 + \epsilon_2^2 . \tag{27}$$

The maximum error occurs when the quantity

$$q = \epsilon_1 \epsilon_2 \left[\ell_1 (m_2 + h n_2) - \ell_2 (m_1 + h n_1) \right]$$

$$- \tau \omega \left[\epsilon_1^2 \ell_1 (m_1 + h n_1) + \epsilon_2^2 \ell_2 (m_2 + h n_2) \right] \tag{28}$$

is a maximum for a given value of ϵ^2. The quantity q is subject to the constraints:

$$\epsilon^2 = \epsilon_1^2 + \epsilon_2^2$$

$$\ell_1^2 + m_1^2 + n_1^2 = 1$$

$$\ell_2^2 + m_2^2 + n_2^2 = 1 \ . \tag{29}$$

Using the method of LaGrange* multipliers, the maximum value of q occurs when

$$n_1 = h m_1$$

$$n_2 = h m_2$$

$$\frac{\epsilon_2^2}{\epsilon_1^2} = \frac{-(1 - 2\ell_1^2)}{(1 - 2\ell_2^2)}$$

$$\frac{\left[(1 + h^2) m_1 m_2 + \ell_1 \ell_2 \right]^2}{(1 - 2\ell_1^2)(1 - 2\ell_2^2)} = -\tau^2 \omega^2 \ . \tag{30}$$

*A discussion of the use of LaGrange multipliers may be found in Ref. 19.

Inspection of this set of equations indicates that there are eight unknowns and only seven equations. However, a re-examination of Eq. (30) indicates that the components of the angular vibration could be written as

$$A_{(I-C)SA} = d' \cos(\omega t + \varphi)$$

$$A_{(I-C)OA} = b' \sin(\omega t + \varphi) + e' \cos(\omega t + \varphi)$$

$$A_{(I-C)IA} = c' \sin(\omega t + \varphi) + f' \cos(\omega t + \varphi) \qquad (31)$$

where the angle φ is dependent only on the instant of time at which the measurement was begun. It is always possible to start this measurement at some instant of time that would make the phase angle φ equal to zero. Since the average error of the instrument given by Eq. (22) must be independent of the time at which the vibration is measured, one of the unknowns in Eq. (30) must be arbitrary. Therefore, set

$$\ell_1 = 0 \ .$$

Substituting the conditions given above, the maximum error in radians per second is:

$$E'_{max} = \frac{\epsilon^2 (1 + h^2)^{1/2} \omega}{4 (1 + \tau^2 \omega^2)^{1/2}} \qquad (32)$$

where ϵ is in radians and τ in seconds of time. Converting to units of arc seconds for ϵ and deg/hr for the error, we have:

$$E_{max} = 1.23 \times 10^{-6} \left[\frac{\omega (1 + h^2)^{1/2} \epsilon^2}{(1 + \tau^2 \omega^2)^{1/2}} \right] . \qquad (33)$$

This maximum possible angular vibration error is plotted as a function of frequency in Figure 17 for two typical gyroscope designs. The instrument with the 0.001 second time constant is used in airborne or ballistic applications and the instrument with the 0.2 second time constant is used in shipboard applications. For a given wheel speed and general design configuration, the ratio of the gyroscope gain to the time constant (h/τ) is relatively constant. The time constant of the instrument is:

$$\tau = \frac{I_{FOA} + I_W}{c_d} \ . \qquad (34)$$

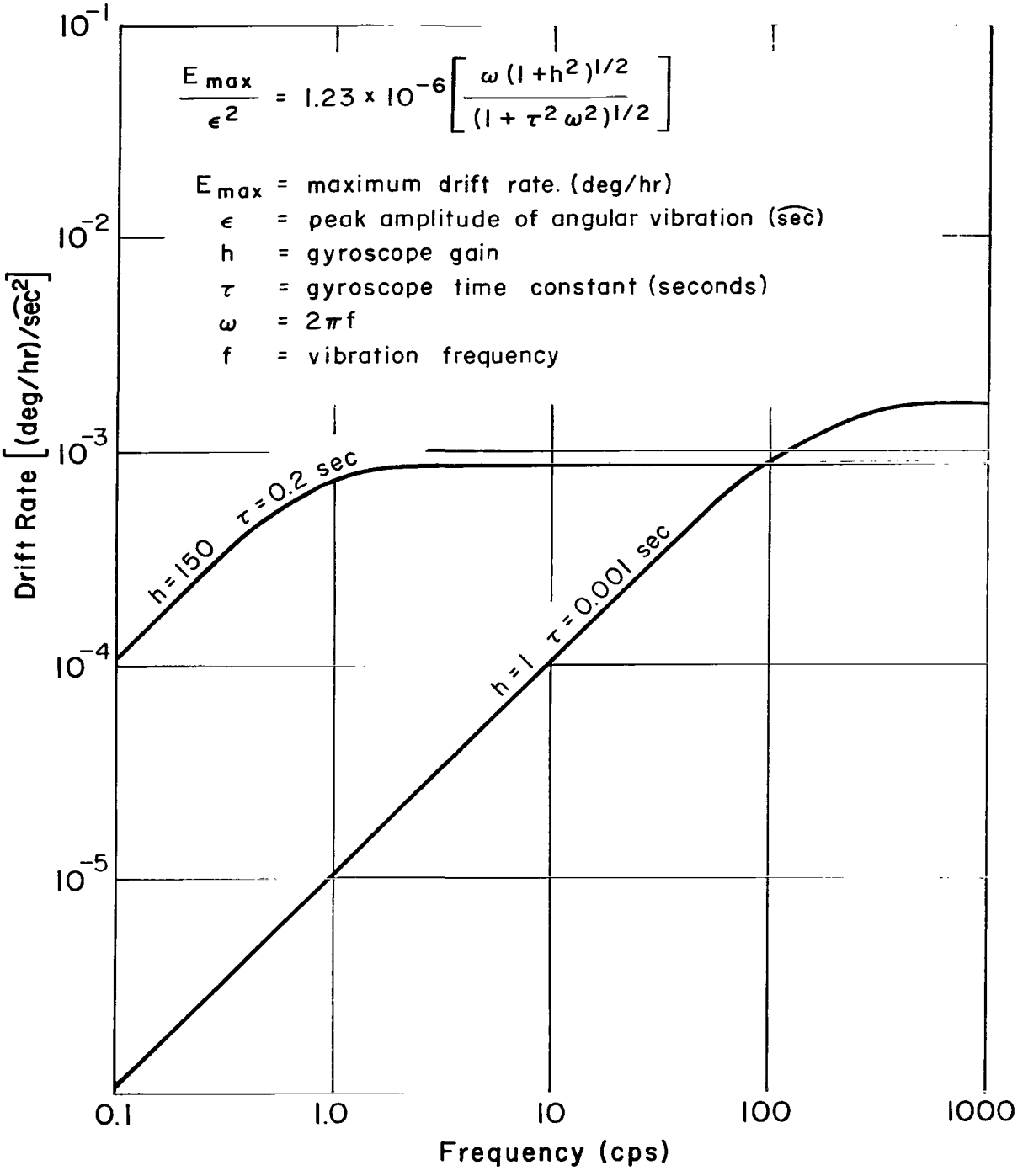

Figure 17.- Maximum steady-state error that may be produced by angular vibration for two typical gyroscope designs--Gyro drift rate versus frequency of vibration

The gain is:

$$h = \frac{H}{c_d} \quad . \tag{35}$$

The ratio is:

$$h/\tau = \frac{H}{I_{FOA} + I_w} \tag{36}$$

The float moments of inertia are proportional to the wheel moment of inertia. The angular momentum H is proportional to the product of wheel speed and wheel moment of inertia. Since at high frequency the angular vibration error is proportional to h/τ, the plots of Figure 17 include a wide range of single-degree-of-freedom rate-integrating instruments. For reference purposes, the sensitivity of rate-integrating gyroscopes to angular vibrations is assumed to be 0.002 deg/hr/sec^2. Two-degree-of-freedom displacement gyros and free rotor gyros are not sensitive to the steady-state angular vibration errors discussed above.

Accelerometer Errors Due to Angular Vibrations

A perfect accelerometer would be insensitive to angular motions. However, many accelerometers are constructed as damped pendulums which at higher frequencies do have sensitivities to angular accelerations. In the simplest instrument, the pendulum is restrained only by gravity and the angular displacement of the float in radians is interpreted as the acceleration along the sensitive axis in g units. (It should be noted that since the operation of this instrument is dependent on gravity, the instrument is not generally useful in space applications.) The equation of motion of this pendulum is given by:

$$I\ddot{\theta} + c_d\dot{\theta} + mgl\,\theta = I\ddot{\theta}_o + mgl\,\theta_o + mla \quad . \tag{37}$$

The solution of this equation of motion is:

$$\left|\theta\right| = \frac{\left|\theta_o\left(1 - \frac{\omega^2}{\omega_n^2}\right) + a/g\right|}{\sqrt{\left(1 - \frac{\omega^2}{\omega_n^2}\right)^2 + 4\beta^2\,\frac{\omega^2}{\omega_n^2}}} \tag{38}$$

where

$$\omega_n = \sqrt{\frac{mgl}{I}}$$

β = ratio of damping to critical

$\omega = 2\pi f$ = circular frequency of vibration.

With the exception of the frequency range near the pendulum natural frequency, the instrument interprets an angular oscillation as an acceleration. Accordingly, an oscillation of 1 arc second is interpreted as a 5 micro-g acceleration. The same arguments that are employed in gyroscope testing, as discussed above, are also used to justify long averaging times for accelerometer data. Averaging times of 10 minutes per data point are not uncommon. For a sinusoidal angular motion, the indicated acceleration is:

$$A_{ind} = 5 \sin \omega t \text{ micro g/sec.}$$

The average acceleration is:

$$\overline{A}_{ind} = \frac{1}{T}\int_{t_1}^{T+t_1} 5 \sin \omega t \, dt = \frac{5}{\omega T}\left[\cos \omega t_1 - \cos \omega (T + t_1)\right] \tag{38a}$$

$$\overline{A}_{ind} = \frac{5}{\omega T}\left[\cos \omega t_1 - \cos \omega t_1 \cos \omega T + \sin \omega t_1 \sin \omega T\right]$$

$$= \frac{5}{\omega T}\left[\cos \omega t_1 (1 - \cos \omega T) + \sin \omega t_1 \sin \omega T\right] . \tag{38b}$$

The mean square indicated acceleration is:

$$\overline{A}^2 = \frac{25}{\omega^2 T^2}\left[\frac{1}{2}(1 - \cos \omega T + \sin \omega T)\right]$$

$$\overline{A}^2_{ind} = \frac{25}{\omega^2 T^2}\left[(1 - \cos \omega T)\right] \tag{38c}$$

The rms indicated acceleration is:

$$\overline{A}_{\text{ind. rms}} = \frac{5}{\omega T}\sqrt{1 - \cos \omega T} \tag{38d}$$

for $\omega T = -1$

$$A_{\text{ind. rms}} = \frac{5\sqrt{2}}{\omega T} \quad . \tag{38e}$$

For averaging times which are long compared to the frequency of vibration, the maximum average indicated acceleration is:

$$\overline{A}_{\text{ind. max}} = \frac{10}{2\pi fT} \text{ micro-g/sec} \tag{38f}$$

The maximum rms indicated average acceleration is:

$$\overline{A}_{\text{ind. rms}} = \frac{7.07}{2\pi fT} \text{ micro-g/sec} \tag{38g}$$

Thus, for an angular vibration of 1 arc second at 1 cps with an averaging time of 10 seconds, the error in acceleration measurement would be of the order of 0.1 micro-g. At frequencies which are low compared to the averaging time the error in indicated acceleration is basically that due to misalignment relative to gravity. More sophisticated pendulum instruments make use of active restraint systems to maintain the pendulum at null. It should be noted that some instruments designed for space use at very low accelerations (10^{-8} g or less) possibly may not have a linear range of more than two or three orders of magnitude. The existence of oscillations representing 10^{-4} g, although at a high frequency, may result in very significant errors due to saturation and other non-linearities in the average indicated acceleration. If it is required that the threshold of measurement be obtained, it is necessary to control the angular oscillations so that the indicated accelerations due to angular vibration must be an order of magnitude smaller than the threshold acceleration as discussed below in the subsection on Accelerometer Errors (page 33). For example, to demonstrate a threshold of 1 micro-g, the indicated acceleration due to angular vibration must be less than 0.1 micro-g. The force required to maintain the pendulum at null is proportional to the acceleration along the sensitive axis of the instrument. The equation of motion of an actively restrained pendulum is:

$$I\ddot{\theta} + c_d\dot{\theta} + mgl\,\theta + K\int_{-\infty}^{t} \theta\,dt = I\ddot{\theta}_o + mgl\,\theta_o + mla \quad . \tag{39}$$

Assuming a solution of the form $Ae^{j\omega t}$ the pendulum angle is:

$$\theta = \frac{j\omega\left[\left(1 - \frac{\omega^2}{\omega_n^2}\right)\theta_o + a/g\right]}{K/mgl + j\omega\left[\left(1 - \frac{\omega^2}{\omega_n^2}\right) + 2\beta j\frac{\omega}{\omega_n}\right]} . \tag{40}$$

Integration and scaling to acceleration units yields the indicated acceleration as:

$$A_{ind} = \frac{K\theta}{mgl}\left(\frac{1}{j\omega}\right) = \frac{\left[\left(1 - \frac{\omega^2}{\omega_n^2}\right)\theta_o + a/g\right]}{1 + j\omega\frac{mgl}{K}\left[\left(1 - \frac{\omega^2}{\omega_n^2}\right) + 2\beta j\frac{\omega}{\omega_n}\right]} . \tag{41}$$

For stability:

$$\frac{K}{mgl} < 2\beta\omega_n .$$

Assuming:

$$\frac{K}{mgl} = 0.5\omega_n, \quad \beta = 0.5$$

The indicated acceleration is:

$$A_{ind} = \frac{\left[\left(1 - \frac{\omega^2}{\omega_n^2}\right)\theta_o + a/g\right]}{1 + \frac{2j\omega}{\omega_n}\left[\left(1 - \frac{\omega^2}{\omega_n^2}\right) + 2\beta j\frac{\omega}{\omega_n}\right]} . \tag{42}$$

The magnitude of the indicated acceleration is:

$$\left|A_{ind}\right| = \frac{\left|\left[\left(1 - \frac{\omega^2}{\omega_n^2}\right)\theta_o + a/g\right]\right|}{\sqrt{\left(1 - \frac{2\omega^2}{\omega_n^2}\right)^2 + \frac{4\omega^2}{\omega_n^2}\left(1 - \frac{\omega^2}{\omega_n^2}\right)^2}} \tag{43}$$

The integration thus acts to filter high-frequency motions; that is, at high frequencies, the sensitivity to angular vibrations is attenuated to produce an error smaller than that associated with the simple pendulum.

Gyroscope Errors Due to Translational Vibrations

If an instrument has a random drift rate of the order 0.0001 deg/hr, it is reasonable to assume that the instrument has been balanced to produce a linear sensitivity to acceleration of less than 0.1 deg/hr/g. Assuming a filter time constant of 10 seconds, at 1 cps, a vibration of 0.01 g would be required to produce a drift rate of the order of 0.00002 deg/hr. This acceleration corresponds to a peak-to-peak displacement of about 0.2 inch. At 0.1 cps, a displacement of 2 inches would be required to produce the same error. At frequencies below 0.015 cps, an acceleration of 0.0001 g (displacements greater than 10 inches) would be required to produce a drift rate of 0.00001 deg/hr. As discussed in the following section, these accelerations are considerably larger than those encountered in measurements of translational vibrations at these frequencies.

Gyroscope instruments also have sensitivities to the square of the applied acceleration known as the compliance or anisoelasticity torque that are very significant in high-acceleration applications. However, assuming a sensitivity of 0.1 deg/hr/g^2, it would require an acceleration of 0.01 g to produce a test error of 0.00001 deg/hr. As discussed in the following section, accelerations of these magnitudes are not encountered in vibration measurements in typical inertial sensor calibration laboratories.

Accelerometer Errors Due to Translational Vibrations

The acceleration due to translational vibrations will be sensed by an accelerometer and, unless the vibration is defined to the accuracy of the instrument, this acceleration will be interpreted as an error. If we are willing to average the acceleration for a period of time T as discussed above, the indicated error due to vibrations whose periods are short compared to the averaging time, the maximum error is:

$$\frac{\left|A_{vib}\right|}{\pi f T} \tag{44a}$$

and the rms error is:

$$\frac{|A_{vib}|}{\sqrt{2\pi}\, fT} . \tag{44b}$$

An acceleration of 10^{-4}g at 1 cps would represent an error with a 10-second averaging time of about 1.5 micro-g. However, if the instrument is not linear, calibration errors will result from the use of averaging, cross correlating, or other smoothing techniques. Consider, for example, the instrument whose idealized signal output is plotted as a function of applied acceleration in Figure 18. At accelerations below the minimum detectable acceleration (threshold) a_o, there is no signal output (this may be due to friction in a pendulum or suspended mass instrument or misalignment errors in an integrating gyroscope accelerometer). At large accelerations, saturation and other non-linearities will limit the signal output at high accelerations. The acceleration under which the instrument is tested is:

$$a = b_o + b_1 \sin \omega t \tag{45}$$

where b_o is the desired input acceleration. If b_1 is of the same order of magnitude as a_o, it is impossible to detect the threshold acceleration a_o. If we assume $b_o = a_o$ and $b_1 = a_o$, the average signal from the instrument is:

$$\overline{S} = \frac{c_1 b_1}{2\pi} \int_o^{\pi} \sin(\omega t)\, d(\omega t) = \frac{c_1 b_1}{\pi} = \frac{c_1 b_o}{\pi} . \tag{46}$$

If $b_1 = a_o$ and $b_o = \frac{a_o}{2}$

$$\overline{S} = \frac{c_1 b_1}{2\pi} \int_{\pi/6}^{5\pi/6} \sin(\omega t)\, d(\omega t) = \frac{0.866\, c_1 b_1}{\pi} . \tag{47}$$

If $b_1 = a_o$ and $b_o = 0$

$$\overline{S} = 0 \tag{48}$$

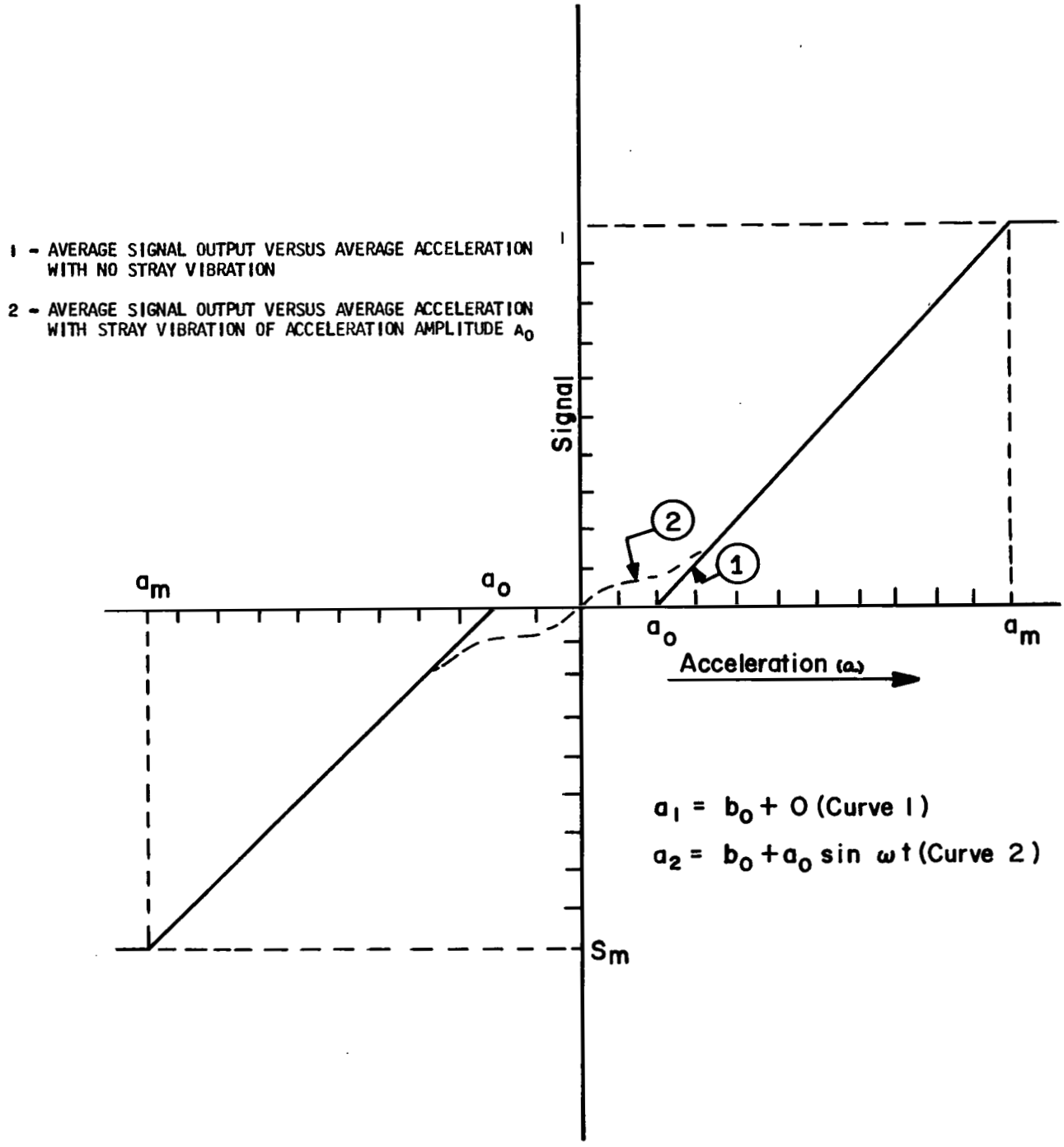

Figure 18.- Idealized accelerometer signal output versus applied acceleration

and if $b_1 = a_o$ and $b_o = 2a_o$

$$\overline{S} = c_1 a_o \quad . \tag{49}$$

The output of the instrument with a vibration of magnitude a_o is plotted as the dashed line of Figure 18. The threshold capability of an instrument may not be determined unless all of the inputs to the instrument are defined to within that accuracy. Thus, to demonstrate a threshold of 1 micro-g, it is necessary to control the environment to 0.1 micro-g.

Summary of Permissible Motions of a Test Platform for Gyroscope Testing

As discussed in the subsection on Gyroscope Errors (page 20), the acceleration sensitivities of a well designed gyroscope instrument are such that accelerations of 0.01 g above 1 cps produce negligible measurement errors after averaging the gyroscope output signal. At lower frequencies the displacements required to produce a significant error are very much larger than those encountered in practice. It is therefore concluded that no translational vibration isolation is required for gyroscope testing. Accordingly a translational vibration of 0.001 g is considered tolerable. Figure 19 plots the errors in gyroscope testing for a 1-arc-second angular vibration for several typical averaging times as a function of vibration frequency. At frequencies below 1 cycle/day, the error is primarily due to misalignment relative to Earth axis. For a 10-second time constant filter or a 20-second averaging time, the error for frequencies between 1 cycle/day and 1 cycle/min is due to the ability of the instrument to measure the instantaneous rate associated with the undesired oscillation. At frequencies above 1 cycle/min, the error is the uncertainty in position error divided by the averaging time Since the errors in this representation are sinusoids and since the inputs have been assumed sinusoidal, the total error due to angular oscillations of ϵ_1 at 10^{-6} cps and ϵ_2 at 1 cps is:

$$E_1 = \sqrt{(7.3 \times 10^{-5})^2 \epsilon_1^2 + (0.1)^2 \epsilon_2^2} \quad . \tag{50}$$

Similarly, if in addition to ϵ_1 and ϵ_2, there is an ϵ_3 at 10^{-4} cps, the total error is:

$$E_1 = \sqrt{(7.3 \times 10^{-5})^2 \epsilon_1^2 + (0.1)^2 \epsilon_2^2 + (2\pi \times 10^{-4})^2 \epsilon_3^2} \quad . \tag{51}$$

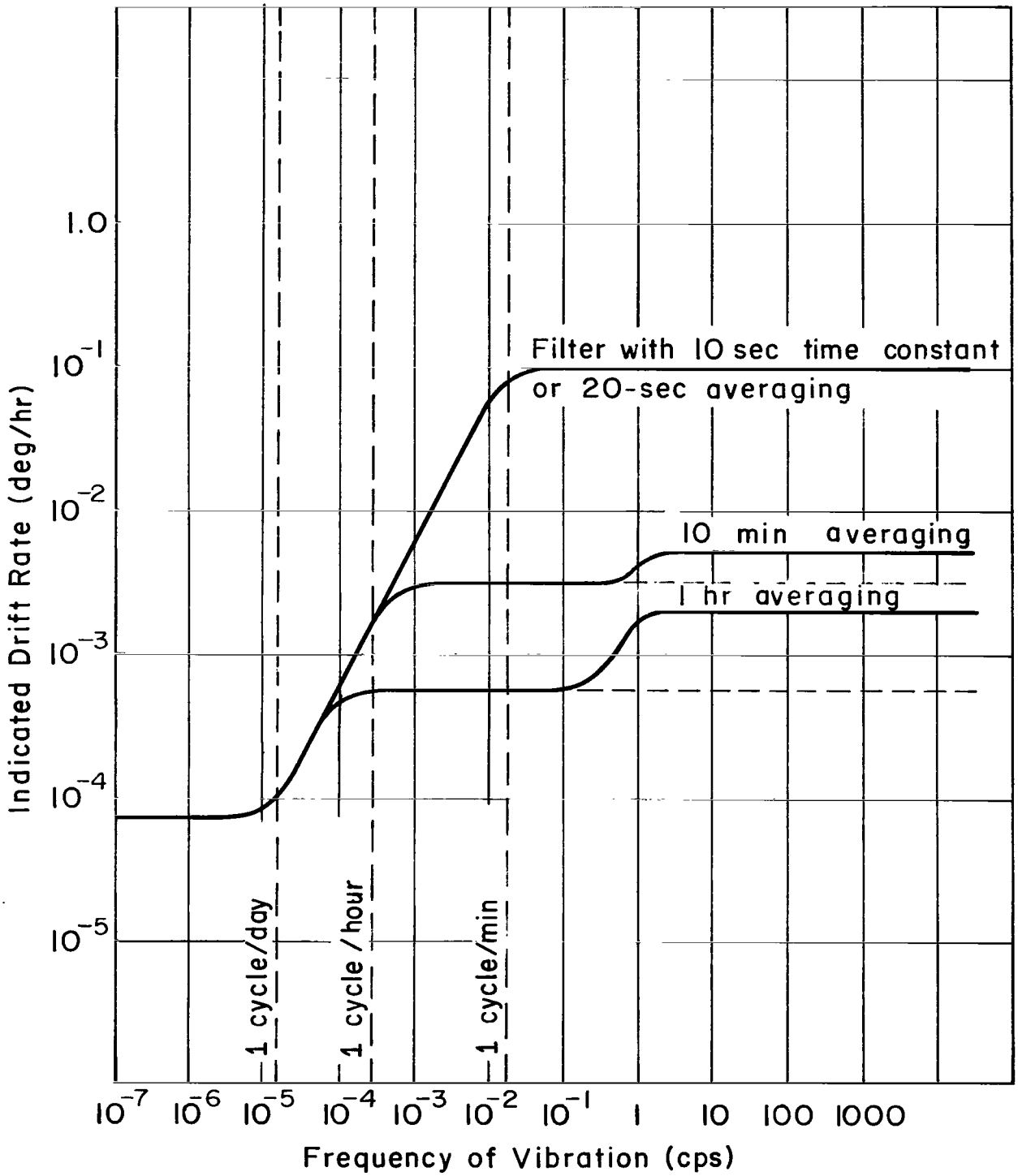

Figure 19.- Maximum error in gyroscope testing due to 1 arc second (vector) angular vibration versus frequency

For the 20-second averaging time, the error due to an angular vibration at a given frequency is approximately given by:

$$e = \frac{(7.3 \times 10^{-5} + 2\pi f)\, \epsilon_f}{\sqrt{1 + (20\pi f)^2}} \quad . \tag{52}$$

The total squared error is then:

$$E^2 = \sum_{i=1}^{n} \frac{(7.3 \times 10^{-5} + 2\pi f_i)^2\, \epsilon_i^2}{1 + (20\pi f)^2} \quad . \tag{52a}$$

If the angular vibration is given as a power spectral density in terms of seconds of arc (peak) squared per cycle per second, the error due to angular vibrations is:

$$E = \sqrt{\int_0^{\infty} \frac{(7.34 \times 10^{-5} + 2\pi f)^2\, \Phi_{\epsilon\epsilon}(f)\, df}{4 + (20\pi f)^2}} \quad . \tag{53}$$

For reference purposes, the tolerable angular motions of the test platform are those which will produce an error no greater than 0.00001 deg/hr. At frequencies below 1 cycle/day, this represents 0.14 arc second. At frequencies above 1 cycle/min, this represents 0.0001 arc second. For permissible errors of 0.0001 deg/hr, the above figures are multiplied by 10 (1.4 and 0.001 arc seconds).

For averaging times of 1 hour, the errors due to angular vibration may be represented as:

$$e = \frac{(7.3 \times 10^{-5} + 2\pi f)\, \epsilon_f}{\sqrt{1 + (3600\pi f)^2}} + \frac{0.002 f\, \epsilon_f^2}{\sqrt{1 + f^2}} \quad . \tag{54}$$

The additional term in the above equation is the steady-state error due to angular vibrations which is negligible for the 20-second averaging time, but may be important

for very long averaging times. If the angular motion is given as the power density spectrum $\Phi_{\epsilon\epsilon}$, the error is:

$$E = \int_0^\infty \frac{2 \times 10^{-3} f \, \Phi_{\epsilon\epsilon}(f)}{\sqrt{1 + f^2}} + \sqrt{\int_0^\infty \frac{(7.3 \times 10^{-5} + 2\pi f)^2 \, \Phi_{\epsilon\epsilon}(f)}{1 + (3600\,\pi f)^2}} \tag{55}$$

At frequencies above 0.0001 cps, an angular motion of 0.18 arc second would produce a drift rate error of 0.0001 deg/hr. If an accuracy of 0.00001 deg/hr is required, the motion must be limited to 0.018 arc second. At these amplitudes the steady-state angular vibration errors are negligible. The error is therefore defined as:

$$E = \sqrt{\int_0^\infty \frac{(7.3 \times 10^{-5} + 2\pi f)^2 \, \Phi_{\epsilon\epsilon}(f)\, df}{1 + (T\pi f)^2}} \tag{56}$$

where T is the effective averaging time in seconds and E is the error in deg/hr.

Permissible Motions of the Test Platform for Accelerometer Testing

If an accelerometer is linear at all accelerations of interest, it is possible to use averaging to obtain the output signal for accelerations less than the acceleration associated with the vibratory output. However, if the instrument has a dead zone (due for example to friction) or other pronounced non-linearity, a vibratory acceleration of the order of the dead zone will act to mask the nature of the non-linearity. Therefore, to measure the threshold in a slightly non-linear instrument, it is necessary to control the vibratory inputs to one-tenth of the desired threshold. Thus, to demonstrate performance at 1 micro-g, it is necessary to control the environment to within 0.1 micro-g. Similarly, for performance measurements at 1 micro-g, it is necessary to know the angle between the accelerometer-sensitive axis and the apparent vertical to within 0.02 arc second.

III. REPRESENTATION OF THE TEST LABORATORY VIBRATION ENVIRONMENT

Introduction

As shown in Section II, angular vibrations and translational vibrations are capable of introducing errors in the calibration of inertial sensors (gyroscopes and accelerometers) if they are of a sufficiently large magnitude. It is the purpose of this section to present an estimate of the vibration environment at a typical urban test laboratory location. It is then demonstrated that the existing vibration environment is too severe to permit the calibration of gyroscope instruments to testing accuracies of 0.1 milli-deg/hr or accelerometers to testing accuracies of 1 micro-g, and that a ground motion isolation system is, in fact, required. As indicated in Sections I and IV, proper design of this isolation system demands at least an approximate description of both the translational and rotational vibrations. The estimates presented here will be supplemented by the following efforts during the course of this study:

1. Air Force Cambridge Research Laboratories, under contract to NASA, Electronics Research Center, will install and operate a semi-permanent seismic test station in the Kendall Square area of Cambridge, Mass. Continuous records will be maintained and analyzed to provide the actual frequency spectrum of translatory ground motions. This contract expires August 19, 1967.

2. NASA Electronics Research Center personnel, with the assistance of the MIT Experimental Astronomy Laboratory, will continue to conduct investigations of instrumentation and techniques for distinguishing between translational and rotational motions. Measurement instrumentation will be installed in the temporary NASA Inertial Test Laboratory at 545 Main Street, Cambridge, Mass., and at the future test site location. The data obtained will be analyzed to provide better estimates of the angular vibration power spectrum. A secondary objective is the design of a measurement system that will permit rapid definition of the basic limitations introduced by laboratory vibration environments. The information presented in the following paragraphs is based on a review of previously existing data and literature and preliminary data obtained by NASA, AFCRL, and M.I.T. Experimental Astronomy Laboratory personnel.

Translational Vibrations

Since the response of the Earth at a given location to an earthquake or other seismic activity is very strongly dependent on local soil structure and, to some degree, the terrain and man-made structures in the area, most seismological data are presented in terms of relative magnitude referenced to the particular location. Until the past 10 years, relatively little quantitative data on the magnitude of the Earth vibrations being measured were reported. The papers are concerned primarily with precise measurements of arrival times of an Earth tremor and the comparison of the apparent propagation velocities with hypotheses of the structural properties of the Earth. Some data have been obtained, especially in California, Japan, and Hawaii, on the vibrations produced by earthquakes. These data were obtained for the engineering design of structures.[20] However, these motions are too infrequent and too severe to be considered

as a representative environment for the test station. Ref. 20 reports acceleration levels during California earthquakes of between 0.04 and 0.33 g. The measurements are made within a 50-mile radius of the earthquake center. Even in seismically active California, the expected average number of major earthquakes is of the order of one per year. [19]

As part of the VELA Uniform program for the detection of nuclear weapons tests, studies have been conducted by the Acoustics and Seismics Laboratory of the University of Michigan to determine the seismic background vibrations of the Earth (vibratory motions that are not associated with any known natural or man-made shock). [21] The results of these studies [22] indicate that the background vibration varies with both time and geographic location. The areas of largest seismic background vibration in the United States are the eastern and western coastal areas. It is believed that major sources of the microseismic activity are ocean waves and meteorological activity. [23] Ref. 22 presents the measured Fourier spectral densities obtained at various test locations in the United States over the frequency range of 0.25 to 100 cps. The results intentionally omit any data that can be attributed to man-made sources. The maximum spectrum is plotted as a power spectral density as Curve A of Figure 20. Curve B obtained from Ref. 24 plots similar data for frequencies between 0.02 and 2 cps. Curve C obtained from Ref. 25 plots vibrations for frequencies between 0.005 and 0.5 cps due to ocean storms as measured at the LaJolla test station of the University of California at San Diego. Efforts were made in all of the above studies to eliminate any man-made disturbances and vibrations caused by the passage of vehicles and other cultural activities. Ref. 20 presents ground motion data obtained within 50 feet of a railroad track that indicates accelerations of the order of 0.03 g due to the passage of a railroad train. Data obtained near a highway indicated accelerations of the order of 0.005 g. Ref. 26 (a study for the Army Guidance and Control Facility at Huntsville, Alabama) presents the frequency spectra caused by vehicles at 75 feet from busy streets in Madison, Wisconsin (Curve F), and Los Angeles, California (Curve E). It is expected that the vibration levels in the Kendall Square Area of Cambridge, Mass., will be more severe than those reported in Ref. 25 because of the high industrial activity in the area. Preliminary data obtained in a building in the area of the NASA-ERC Inertial Sensor Test Laboratory are reported in Ref. 27. Rms background vibration levels of the order of 35 to 70 micro-g at frequencies near 5 cps were observed during normal working hours. Trains passing through the area produced peak accelerations as large as 115 micro-g. Preliminary data obtained by AFCRL also give acceleration values of the order of 100 micro-g between 3 and 6 cps. The reference power spectrum of Figure 20 indicates an acceleration level of approximately 470 micro-g (rms) in the band between 3 and 25 cps. The reference plot assumes a white noise displacement of 0.1 thousandths of an inch squared per cps (0.1×10^{-6} in.^{2}/cps) for frequencies between 0.01 and 0.1 cps, a white noise velocity from 0.1 cps to 3 cps, and a white noise acceleration to 25 cps. The spectrum is then assumed to fall off at 3-1/3 orders of magnitude per decade. At frequencies below 0.005 cps, the only quantitative measured data found available have been obtained by strain measurements during the Chilean earthquake of 1960 and the Alaskan earthquake of 1964. The plot D is obtained by estimating the displacement as the measured strain [28] for the Alaskan earthquake multiplied by the radius of the Earth and converting to acceleration units. It appears reasonable to assume that the normal vibration levels will be orders of magnitude below this estimate. The heavenly bodies (planets, the moon, the sun, and other stars) all exert gravitational forces on the Earth. The size of the Earth and its rotation about its own axis and motions relative to the other celestial bodies result in a

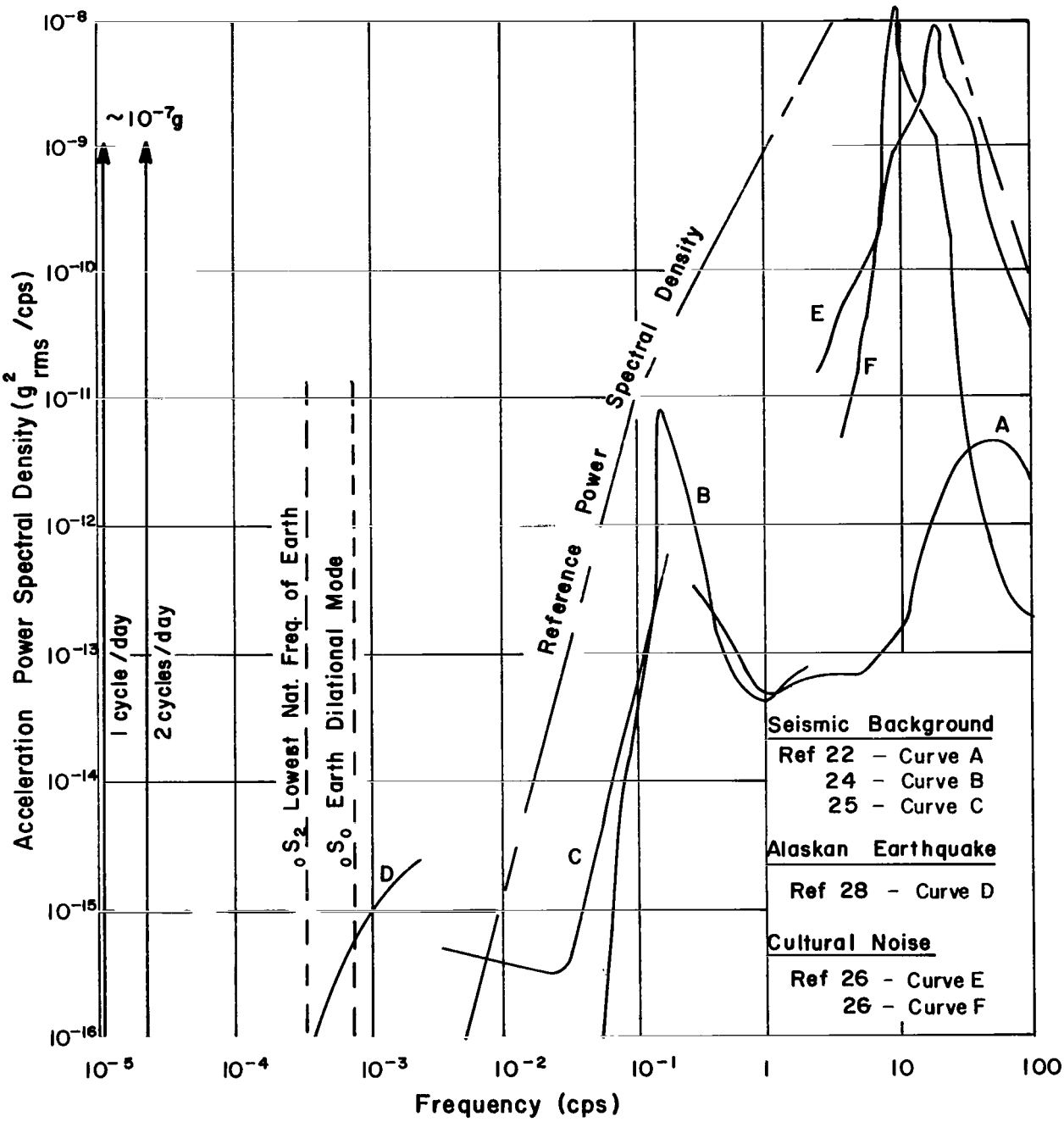

Figure 20.- Representative acceleration power spectral density for test station

variation of gravity as a function of time and position on the surface of the Earth. This variation in the gravity field has a magnitude of the order of 0.1 micro-g[29] and a primary frequency of 2 cycle/day. There are also components at all the frequencies associated with the gross motion of the Earth (i.e., 1 cycle/day, 1 cycle/29 days, 1 cycle/year, etc.) which change the amplitude of the 2-cycle/day variation. This specific force variation results in the ocean and Earth tides. An estimate of the displacement of the Earth caused by these specific force variations is of the order of 1 foot.[30] At frequencies between 2 cycle/day and 0.01 cps, a white noise displacement of 0.1×10^{-6} in.^{2}/cps is probably too small. For purposes of this estimate we assume a white noise acceleration spectrum of $10^{-15}g^2$/cps from 0 to 0.01 cps.

Tilts and Angular Vibrations

With the exception of the scattered measurements reported in Ref. 1, no available data have been located in the literature describing the angular vibrations of typical test stations. Ref. 1 quotes tilts of the following magnitudes: 90 sec/yr, 5 sec/mo, 15 sec/wk, 22 sec/48 hr, 22 sec/day, and 11 sec/6 hr. Possible causes for these motions include: solar heating, non-uniform heating in the structure, local soil conditions, and live loads in the building structure. No data which provide a frequency spectrum of the angular vibrations have been located. Accurate measurements of azimuth variations appear to be non-existent for periods shorter than several months. Several measurements have been made of tilt motions in the vicinity of the site of the NASA-ERC Inertial Test Laboratory at test locations within the MIT Instrumentation Laboratory. Figure 21 presents data obtained by MIT Instrumentation Laboratory personnel at a test location in a building at 224 Albany Street in Cambridge, Mass. During working days (Monday through Friday), there is a daily variation in level of about 5 arc seconds peak-to-peak with instantaneous rates which are quite large compared to the reference slope of 0.1 millideg/hr. This would prohibit the use of this test station for measurements of gyroscope performance to this accuracy. It should be noted that the tilts cannot be attributed to natural sources (e.g., solar heating), since the variation in level diminishes considerably over the weekend (Saturday and Sunday). A plausible explanation for these tilts would be a visco-elastic behavior of the soil structure of the building. Personnel enter the building between 8 and 9 a.m. and the building remains occupied until about 5 p.m. The load on the building causes it to settle continuously until 5 p.m. when the load is removed. The building then returns slowly to its unloaded state. This hypothesis is confirmed somewhat by the regular discontinuity at 12 noon (lunch time) when part of the building load is removed for about an hour. Although, by consideration of local soil conditions and by structural design, it may be possible to reduce or minimize the effects of local activity on building tilts, the mechanism of the tilts is not the concern of this memorandum. The efforts here are restricted to definition of the magnitudes and frequencies of possible rotational disturbances to provide a representation of the environment in which a base motion isolation system must function.

An estimate of the maximum possible angular vibration spectrum that can exist is obtained from the reference acceleration spectrum. If we assume a rigid test fixture whose base is a 10-inch circle and that the center of the circle is fixed but there is a rigid body rotation of θ' radians, the acceleration at the edge of the base is:

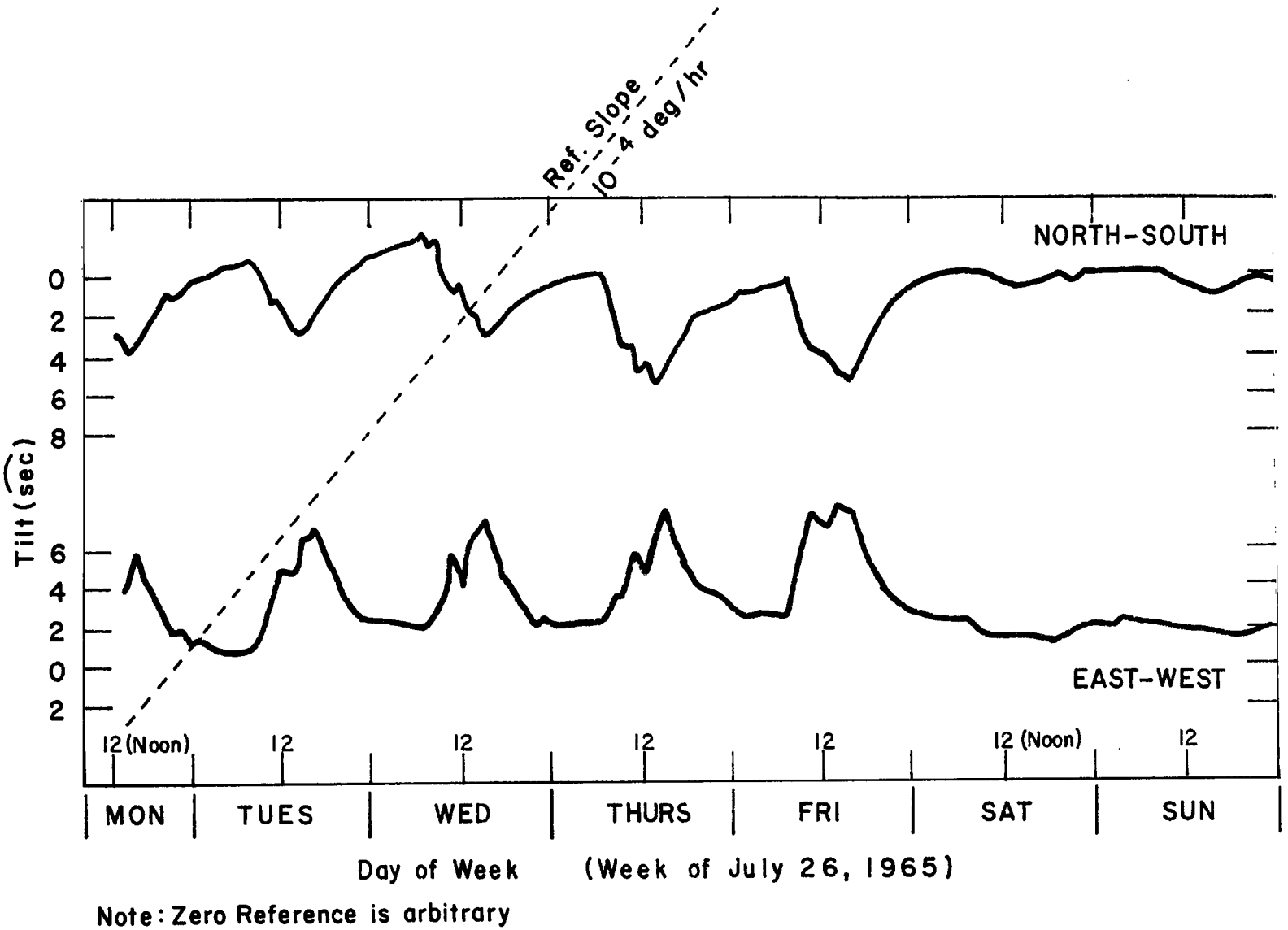

Figure 21.- Tilt of test station at MIT Instrumentation Laboratory basement located at 224 Albany St., Cambridge, Mass.--Data obtained by D. Swanson of Instrumentation Laboratory

$$a = \frac{5\,(2\pi f)^2\,\theta'}{386}\,. \tag{57}$$

If θ is the angle in arc seconds:

$$a = \frac{5\,(2\pi f)^2\,\theta}{(386)\times(2.06\times 10^5)}\ g$$

$$= 2.48\,f^2\,\theta\times 10^{-6}\ g\,. \tag{58}$$

If $\Phi_{aa}(f)$ is the acceleration power spectral density, the angular vibration power spectral density $\Phi^*_{\theta\theta}(f)$ must be less than:

$$\Phi_{\theta\theta}(f) < \frac{\Phi_{aa}(f)\times 10^{12}}{6.15\,f^4} \tag{59}$$

Thus, at 100 cps, the maximum possible angular spectral density is:

$$\Phi_{\theta\theta}(100) < \frac{10^{-10}\times 10^{12}}{6.15\times 10^8}$$

$$< 1.63\times 10^{-7}\ \widehat{\text{sec}}^2/\text{cps}. \tag{60}$$

At 25 cps:

$$\Phi_{\theta\theta}(25) < \frac{10^{-8}\times 10^{12}}{6.15\times(25)^4} = 4.16\times 10^{-3}\ \widehat{\text{sec}}^2/\text{cps} \tag{61}$$

At 3 cps:

$$\Phi_{\theta\theta}(3) < \frac{10^{-8}\times 10^{12}}{6.15\times 34} = 2.06\ \widehat{\text{sec}}^2/\text{cps}. \tag{62}$$

This maximum spectrum is plotted as the upper bound of Figure 22. A second estimate may be made by assuming that the vibration may be represented as a propagating wave in an elastic half-space where the vertical displacement is given as:

$$Z = Z_o \sin\left[\frac{2\pi x}{\lambda} - 2\pi ft\right] \tag{63}$$

The wavelength λ is related to the frequency of vibration by:

$$\lambda = v/f$$

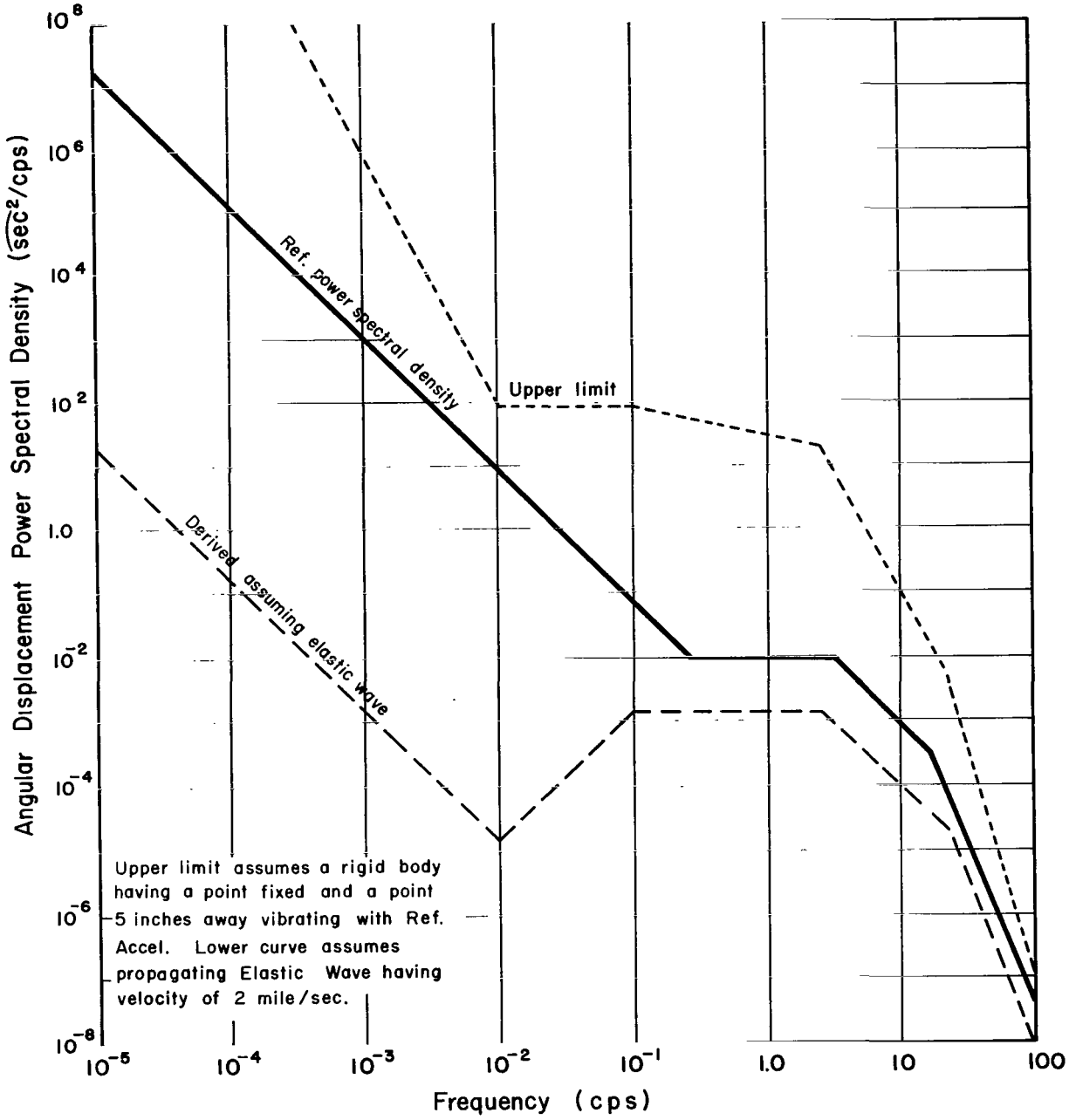

Figure 22.- Estimated angular displacement power spectral density obtained from reference acceleration spectrum

where v is the velocity of propagation in the material. The angular motion is the slope of the surface wave:

$$\theta' = Z_o \frac{2\pi f}{v_o} \cos\left[\frac{2\pi f}{v_o} x - 2\pi ft\right] \tag{64}$$

Converting to units of acceleration in g and arc seconds:

$$\theta = \frac{a_Z g}{2\pi f v_o} \cos\left[\frac{2\pi f}{v_o} x - 2\pi ft\right] \times 2.06 \times 10^5 \tag{65}$$

and assuming $v_o \approx 2$ miles/sec (see Ref. 31):

$$|\theta| = \frac{386\, a_Z\, (2.06 \times 10^5)}{(2\pi f)\,(2 \times 5{,}280)}$$

$$= \frac{1.2\, a_Z \times 10^3}{f} \cdot \tag{66}$$

The power spectral density of the angular rotation is:

$$\Phi_{\theta\theta}(f) = \frac{1.44\, \Phi_{aa}(f) \times 10^6}{f^2} \cdot \tag{67}$$

At 100 cps the angular rotation would be:

$$\Phi_{\theta\theta}(100) = \frac{1.44 \times 10^{-10} \times 10^6}{10^4}$$

$$= 1.44 \times 10^{-8}\ \widehat{\text{sec}}^2/\text{cps} \cdot \tag{68}$$

At 25 cps:

$$\Phi_{\theta\theta}(25) = \frac{1.44 \times 10^{-8} \times 10^{+6}}{(25)^2}$$

$$= 2.3 \times 10^{-5}\ \widehat{\text{sec}}^2/\text{cps}. \tag{69}$$

At 3 cps:

$$\Phi_{\theta\theta}(3) = \frac{1.44 \times 10^{-8} \times 10^{6}}{(3)^{2}}$$

$$= 1.6 \times 10^{-3} \widehat{\text{sec}}^2/\text{cps}. \qquad (70)$$

This power spectrum is plotted as the lower bound of Figure 22 and is derived from the reference acceleration power spectral density.

Neither of the above power spectra are valid representations of the angular vibration environment. The upper limit curve assumes that the wavelength of the vibration is short compared to 5 inches at all frequencies and that structures of a size larger than 10 inches cannot be made rigid. The upper limit curve does, however, represent a maximum possible angular vibration consistent with the reference acceleration spectrum. If the soil, structure, and test platform were, in fact, part of a semi-infinite elastic space with properties that are independent of frequency and amplitude, the lower power spectrum would be a fair respresentation. However, at very low frequencies soils do not behave as elastic materials and tend to exhibit viscous and visco-elastic behavior. This effectively results in a decrease in the velocity of wave propagation and permits larger angular motions. At higher frequencies the structures and soil variations at a particular location may result in amplifications of the angular motions above those to be expected in an elastic half-space. The reference spectrum shown in Figure 22 is estimated from the above considerations and the scattered measurements reported in the literature. At frequencies below 10^{-5} cps, the spectrum is assumed to have a constant value of 10^{8} $\widehat{\text{sec}}^2$/cps. At frequencies of the order of 1 cycle/day, this implies an rms angular displacement of about 30 arc seconds which is the same general order of magnitude as the 10 arc second peak-to-peak variation shown in Figure 7 and the 22 arc seconds reported in Ref. 1. At a frequency of 0.01 cps, the reference spectrum indicates angles of about 0.3 arc second rms which is consistent with the 1-arc-second transient shown in Figure 8. At frequencies above 0.3 cps, there is only a factor of 3 margin between the rms of the reference displacement spectrum and that predicted by the elastic wave since it is felt that the soil and structure do behave elastically at frequencies above 0.3 cps.

Measurement of the Vibration Environment

The reference translational and angular vibration spectra discussed above are based on worst-case estimates which combine measurements at various locations and under various conditions. Given a particular test location, it is preferable to use data measured at that location for evaluating the effects of vibration on an inertial sensor test or to design a base motion isolation system if it is required. As of this date, no reports have been issued by Air Force Cambridge Research Laboratories on measurements at the site of the NASA-ERC Inertial Test Facility. The following paragraphs describe efforts made to date by NASA and MIT Experimental Astronomy Laboratory (EAL) at assembling and evaluating instrumentation for determining the environment at the facility site.

Two horizontal and two vertical seismometers, designed and constructed by the Geosciences Division of Texas Instruments, have been borrowed from the Weston Seismological Observatory of Boston College with the consent of Air Force Cambridge Research Laboratories. Preliminary data (Figures 23 and 24) indicate that these instruments can be used to measure angular motions of a test station as well as provide data on the translational vibration spectrum for frequencies above 0.1 cps. The data shown in Figures 23 and 24 were obtained by mounting two vertical seismometers side-by-side on the floor of the EAL test lab. The seismometer outputs were then amplified and passed through a differential amplifier as shown schematically in Figure 25. The amplification of the seismometers before the differencing of the signal was adjusted to provide a minimum output signal. One of the seismometers was then displaced in 1-meter intervals from the other seismometer. The change of the seismometer output per unit displacement (the slope of the curves) is the angular velocity of the floor in the frequency range between 1 and 30 cps. The frequency spectrum of the seismometer indicated angular velocities will be obtained at the temporary NASA laboratory at 545 Technology Square and at the site of the future test laboratory. Similar measurements will be made using the horizontal seismometers.

Tests are also in progress to determine the applicability of the Kearfott T2503 (surplus equipment from the Atlas guidance system) gyroscope for measurement of the angular vibration spectrum. Preliminary data (see Figure 26) obtained with the gyro operating in a rate feedback mode (Figure 27) indicate a rate of the same order of magnitude as that indicated by the seismometers. The differences between the two results are due, in part, to the difference in locations of the measurements and differences in the filter characteristics of the two measuring systems. Figure 26 plots the indicated rate measured by the gyroscope as a function of time for two successive days. It should be noted that the change of angular rate with time corresponds closely to the simultaneous measurement of the vibratory accelerations shown in Figure 28. The acceleration was measured with a pendulous electronic level (Talyval) manufactured by Taylor Hobson, Ltd. This instrument has not been calibrated as an accelerometer or angle sensor for vibratory motions. A fixture for calibrating the frequency response of this instrument is being constructed by EAL. This calibration is required to evaluate previous data obtained with these instruments. The Talyval instrument has the advantage of small size and weight compared to most seismometers.

In addition to constructing the test fixture for calibrating the Talyval instrument, EAL will assemble a measurement system consisting of two horizontal and two vertical seismometers and two gyroscope instruments with appropriate electronics and instrumentation to permit continuous monitoring of the translational and rotational vibration spectrum. Estimates of the vibration spectrum at EAL will be obtained to demonstrate the capabilities of the system before installation in the Technology Square Laboratory. The Talyval instruments will be used to obtain measurements of long-term tilts of the laboratory floor. The measurements at Technology Square and later at the future laboratory site will be used to improve the reference spectra shown in Figures 20 and 22.

Effect of Reference Vibration Environment on Accelerometer Testing

As discussed in Section II, it is impossible to demonstrate an accelerometer threshold that is smaller than the peak acceleration of the environment in which it is tested. The

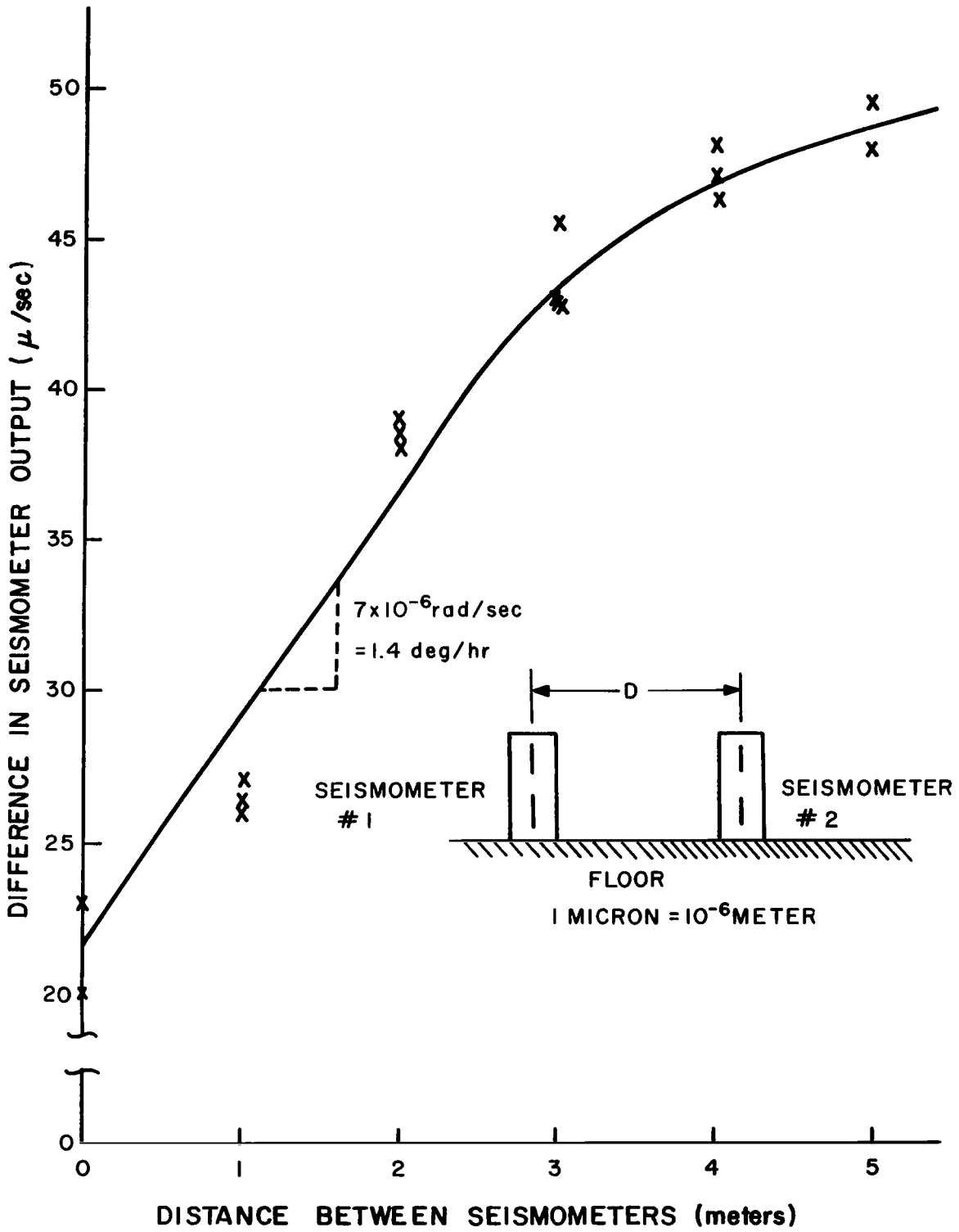

Figure 23.- Measurement of angular velocity of floor in room 325, MIT, Bldg. N-53--Measurements made using two vertical seismometers from 10:00 a.m. to 12 noon on 20 April 1966

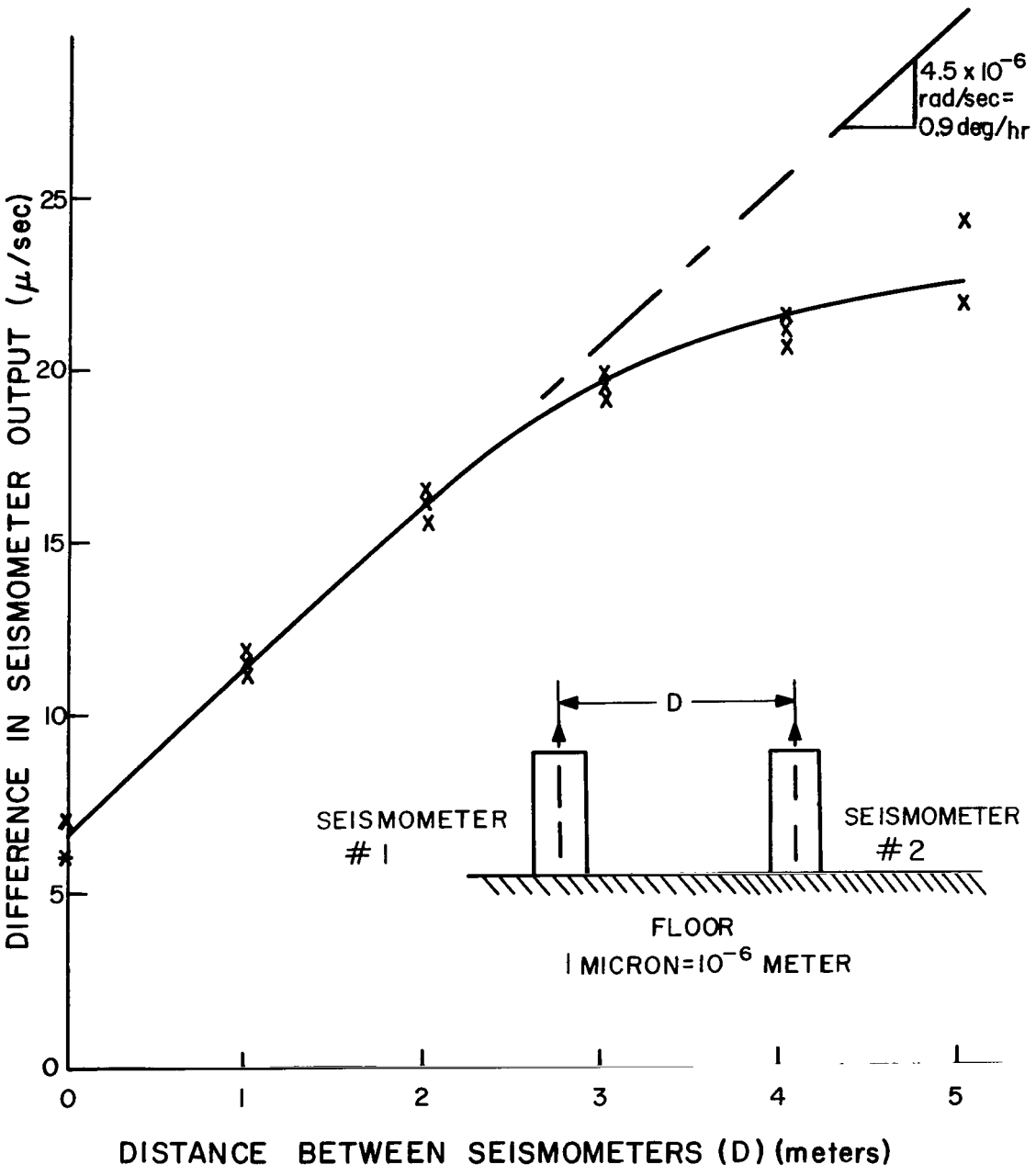

Figure 24.- Measurement of vibratory angular velocity of floor of room 325 of MIT Bldg. N-51--Measurements made using two vertical seismometers at 3:30 p.m. on April 4, 1966

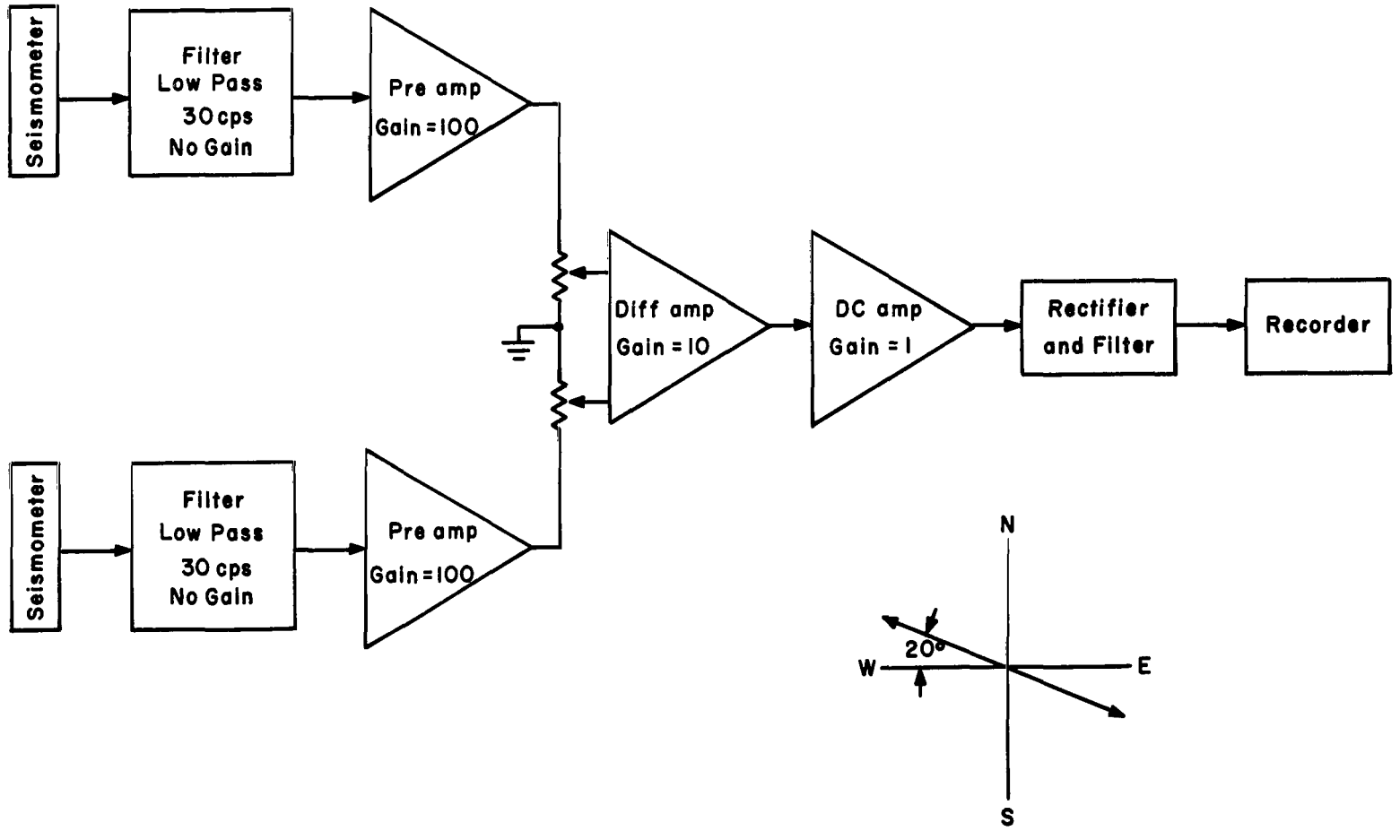

Figure 25.- Block diagram of seismometer run -- 10:00 a.m., April 20, 1966

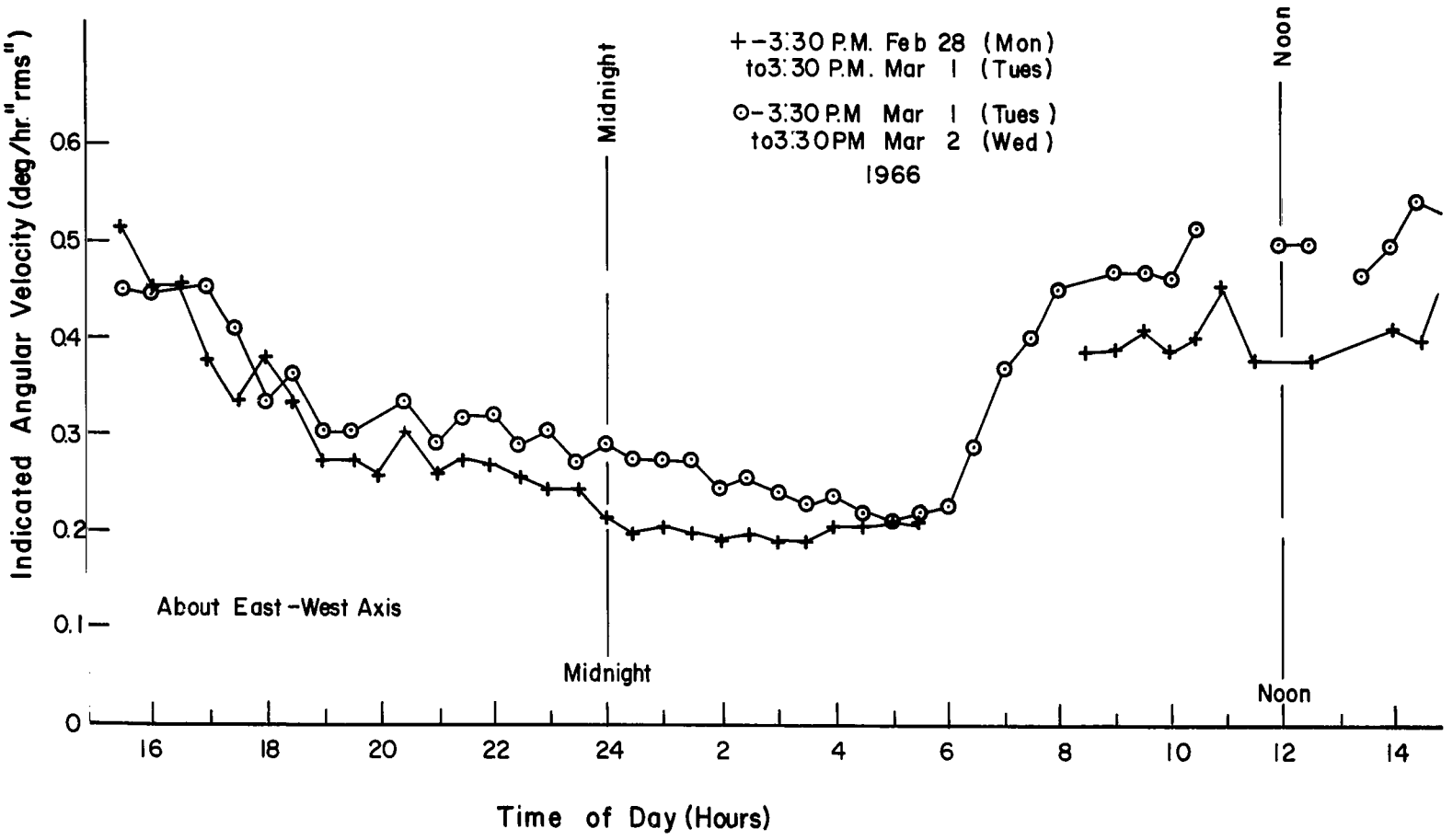

Figure 26.- RMS indicated angular velocity of test station at MIT Experimental Astronomy Laboratory, MIT Bldg. N-51, room 325, February 28 to March 2, 1966--Filtered using bandpass filter set to admit between 0.1 and 10 cps--Rate measured by Kearfott T2503 2A gyroscope, Ser. #298

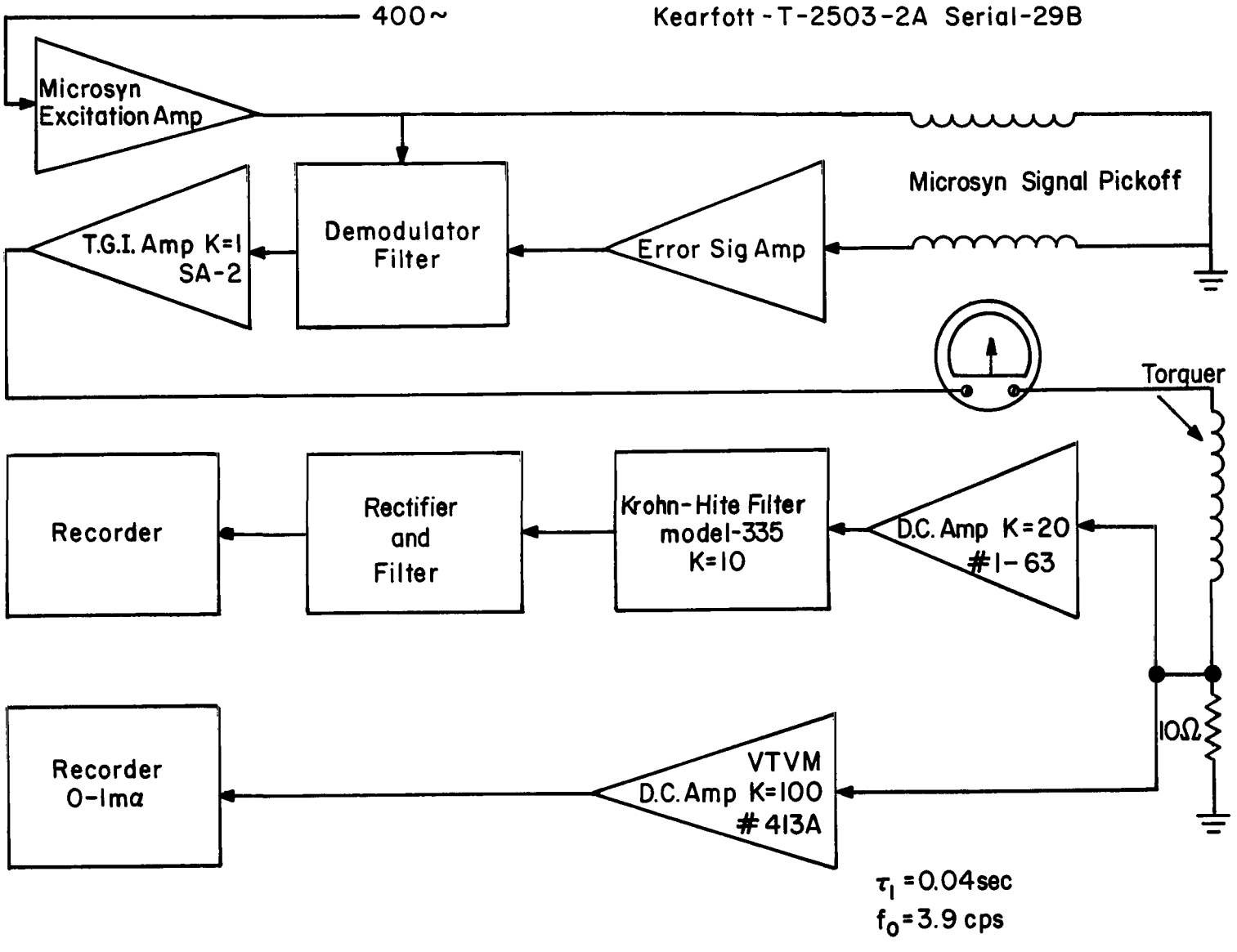

Figure 27.- Block diagram of gyroscope loop used for angular vibration measurement

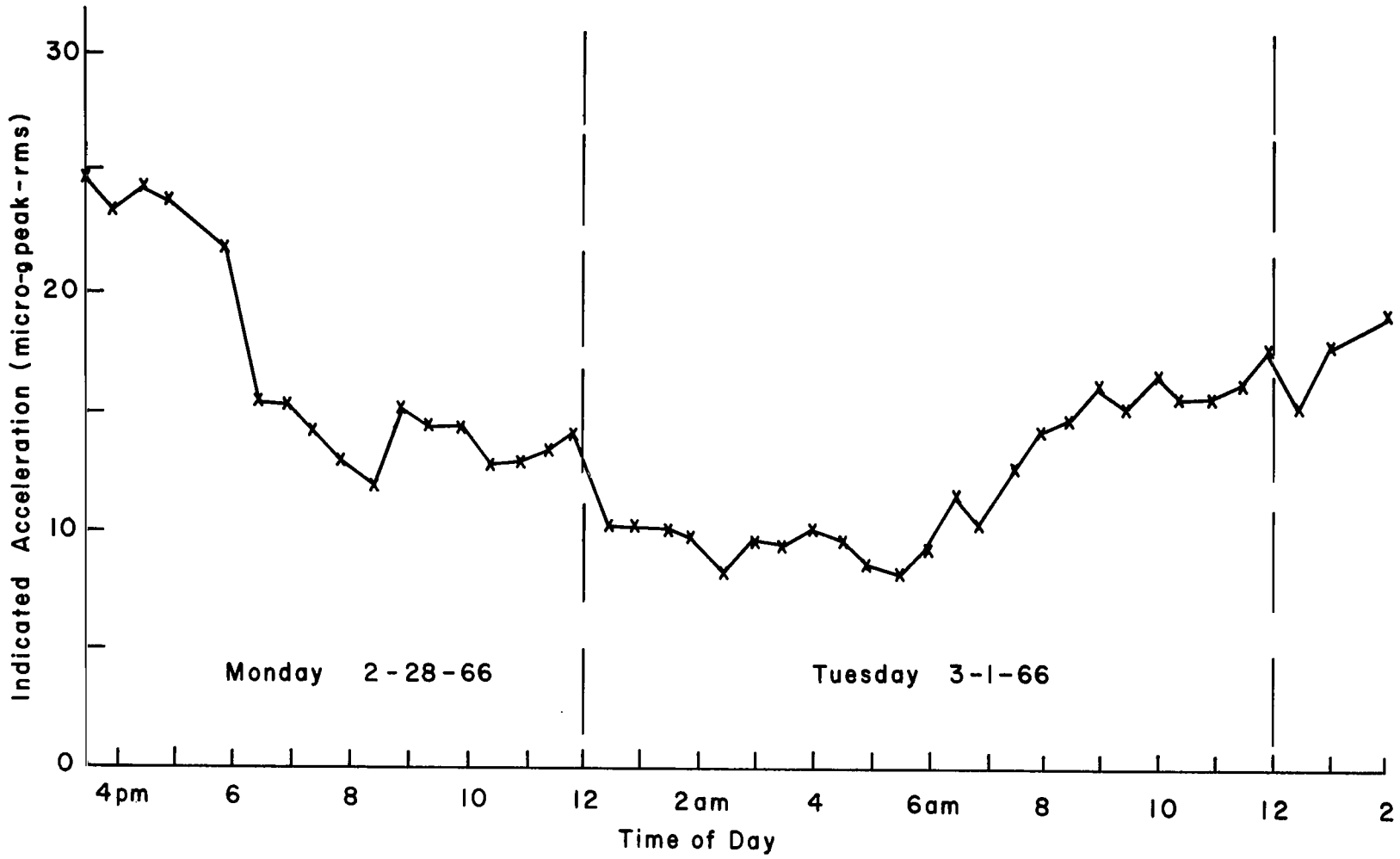

Figure 28.- Indicated acceleration of test station at MIT Experimental Astronomy Laboratory, room 325, Bldg. N-51, February 28 to March 1, 1966

mean squared acceleration of the reference translation spectrum (neglecting gravitational effects) is:

$$\bar{A}^2 = 10^{-17} + 10^{-15}\int_{10^{-2}}^{10^{-1}} (f/10^{-2})^4\, df + 10^{-11}\int_{10^{-1}}^{3.16} (f/10^{-1})^2\, df$$

$$+ 22 \times 10^{-8} + 10^{-8}\int_{25}^{\infty} (f/25)^{-3.33}\, df$$

$$= 10^{-17} + 0.2 \times 10^{-12} + 1.05 \times 10^{-8} + 22 \times 10^{-8} + 10.8 \times 10^{-8} \simeq 34 \times 10^{-8}\, g^2 \tag{71}$$

The rms acceleration is about 580 micro-g. In this environment, a threshold measurement of 0.001 g would be impossible. If we are willing to assume accelerometer linearity and the test objective is to determine the instrument bias or scale factor, common practice would be to average the data for a finite period of time. For an averaging time T, Section II gives the error for a single frequency acceleration of peak magnitude A_o as:

$$e_{rms} = \frac{A_o}{2\pi fT}\sqrt{1 - \cos 2\pi fT} \quad . \tag{72}$$

The mean squared error due to the spectrum of Figure 20 is:

$$E^2 = \frac{1}{2\pi^2 T^2}\int_0^{\infty} \frac{\Phi_{aa}(f)\,(1-\cos 2\pi fT)\, df}{f2} \quad . \tag{73}$$

Since this function is difficult to evaluate, for purposes of approximation, we set:

$$1 - \cos 2\pi fT = \frac{(2\pi fT)^2}{2} \quad \text{for } fT \le 1/2 \tag{74}$$

and $(1 - \cos 2\pi fT) = 2$ for $fT > 1/2$.

These approximations will result in an estimated error that is too large. For an averaging time of 50 seconds, the estimated mean squared error neglecting long period variations in gravity is:

$$E^2 \approx 10^{-17} + \frac{1}{2\pi^2 T^2}\int_{10^{-2}}^{10^{-1}} \frac{10^{-15}}{f^2}\left(\frac{f}{10^{-2}}\right)^4 df$$

$$+ \frac{1}{2\pi^2 T^2} \int_{10^{-1}}^{3.16} \frac{10^{-11}}{f^2} \left(\frac{f}{10^{-1}}\right)^2 df$$

$$+ \frac{1}{2\pi^2 T^2} \int_{3.16}^{25} \frac{10^{-8}}{f^2} df + \frac{1}{2\pi^2 T^2} \int_{25}^{\infty} \frac{10^{-8}}{f^2} \left(\frac{f}{25}\right)^{-3.33}$$

$$= 10^{-17} + \frac{1}{2\pi^2 T^2} (5.9 \times 10^{-9}) = 0.12 \times 10^{-12} \, g^2 \qquad (75)$$

For an averaging time of 50 seconds, the rms error is therefore about 0.35 micro-g. For an averaging time of 5 seconds, the error would be near 3.5 micro-g for this severe translational vibration spectrum.

If, however, it is necessary to show that the bias is constant over a long time period, the angular tilts and vibrations will produce more significant errors. For periods of the order of 12 hours, Figure 22 indicates variations in tilt of about 30 arc seconds which would be a 150-micro-g error. At frequencies of about 1 cycle/hr, the reference spectrum indicates about 3 arc seconds and an associated error of 15 micro-g. It should be noted that the higher frequency angular vibrations (above 0.1 cps) of the reference spectrum produce negligible indicated accelerations when compared to the reference translational acceleration spectrum.

Effect of Reference Vibration Spectra on Gyroscope Testing

As discussed in Section II (Gyroscope Errors), an instrument with an acceleration sensitivity of 0.1 deg/hr/g, tested with a 10-second filter, would require an acceleration of 5000 micro-g at 1 cps to produce an error of 0.1 millideg/hr. The 580 micro-g acceleration obtained from the reference spectrum should therefore introduce negligible errors (especially since most of the energy is contained above 3 cps).

The error for gyroscope testing due to angular vibrations is calculated in the manner indicated in Section II and the error resulting from the angular vibrations in each decade frequency band is tabulated in Table I.

It should be noted that for tests with long filtering times (several minutes or more), the most significant errors are produced by the portion of the spectrum below 0.001 cps. For tests with shorter, averaging times, however, the spectrum at higher frequencies must be taken into account.

TABLE I

ERROR IN GYROSCOPE TESTING
PRODUCED BY REFERENCE ANGULAR VIBRATION SPECTRUM
FOR SEVERAL FILTERING TIMES
(millideg/hr (rms))

Frequency Band (cps)	Filter Time Constant (τ)			
	Seconds		Minutes	
	10	30	10	30
$0\text{-}10^{-5}$	2.3	2.3	2.3	2.3
$10^{-5}\text{-}10^{-4}$	4.9	4.9	4.9	4.5
$10^{-4}\text{-}10^{-3}$	11.7	11.7	11.2	3.6
$10^{-3}\text{-}10^{-2}$	20.3	20.0	2.5	0.8
$10^{-2}\text{-}10^{-1}$	35.6	12.2	0.6	0.2
$10^{-1}\text{-}1.0$	11.2	3.7	0.2	0.06
1-10	20.8	7.0	0.35	0.12
10-100	8.1	2.7	0.14	0.05
Total	51	28	12.7	6.1

IV. DESIGN CONSIDERATIONS

Gyroscope Test Station

As discussed in Section I, the bandpass of the MIT Instrumentation Laboratory servo-levelled platform is limited by the effect of the translational vibration environment on the control transducer. It is believed that a considerable improvement can be made in the performance of this system by the use of additional control sensors (perhaps, by the addition of a gyroscope instrument as indicated in Figure 29). In this system, the accelerometer or level vial would maintain control for low frequencies until the disturbances due to translational vibration become significant. At higher frequencies, the gyro instrument would assume control. As the frequency is increased further, noise signals from the gyroscope instrument become large in comparison to the desired control signal. At these frequencies, and higher, it would be desirable to fix the system to the floor and accept the ambient environment. The statement of the analytical design problem is to find the values of the parameters (e.g., τa, K, τg) and filter characteristics L_1, L_2, and G that cause the rms error E defined in Section II to be a minimum; that is, the quantity:

$$E = \sqrt{\int_0^\infty \frac{\left[7.3 \times 10^{-5} + (2\pi f)\right]^2 \Phi_{\delta\delta}(f)\, df}{(1 + (2\pi f \tau))^2}} \qquad (76)$$

where $\Phi_{\delta\delta}$ is the power spectral density of the error angle δ in seconds of arc squared per cps and τ is the averaging time for the gyroscope test. Rather than accepting the ambient environment of the laboratory at high frequencies, it may be advantageous to use inertia isolation possibly as indicated in Figures 30 and 31. In this system the analytical design objective is not so readily defined. A solution of I approaching infinity and ω_θ approaching zero would satisfy the mathematical condition but is meaningless in a practical sense except to say that for passive isolation a very large mass and a low natural frequency are desirable. If, however, the mass of the platform and its moment of inertia are fixed arbitrarily, the optimum design for a given sensor combination can be analytically determined if the disturbance forces and instrumentation errors can be quantitatively defined. At frequencies above the active control system cutoff frequency, the design decision is a choice between passive isolation and acceptance of the ambient environment. Figure 31 permits both of these alternatives in that, if the natural frequency ω_θ is infinite, the passive isolation disappears and Figures 29 and 31 become equivalent. At frequencies below the active control cutoff frequency, the system is limited by the ability of the control sensors to produce a signal v that is primarily a function of the error angle and is not contaminated by noise signals due to instrument errors and disturbances.

The next phase of this study of the design of a platform for gyroscope testing is the determination of those control sensors, which are currently available, and their accuracies and error models. The best set of control sensors and the best means of combining their output signals to obtain the best control signal v for indicating the error

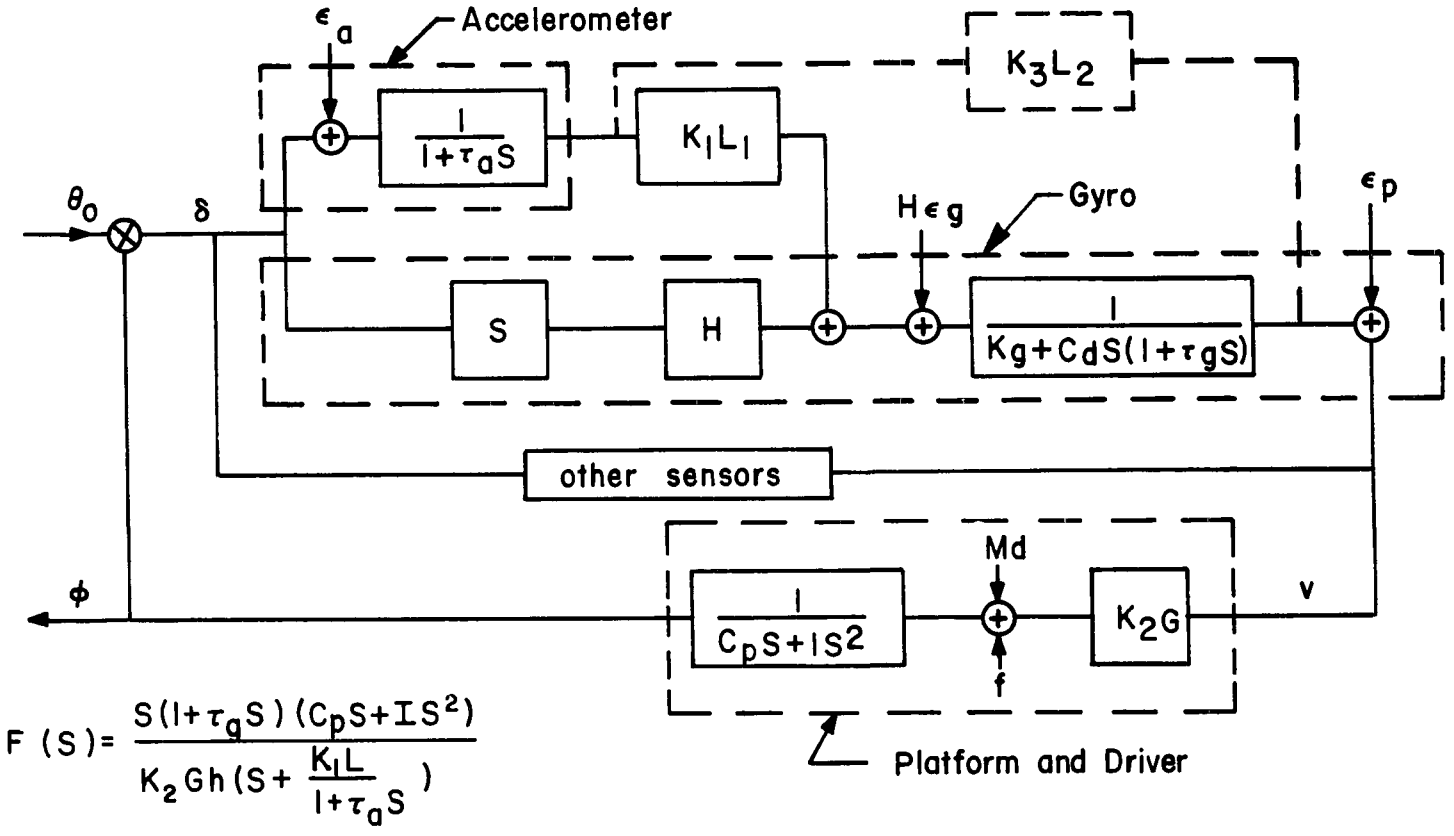

No Passive Isolation

$$\delta=\frac{1}{1+F(S)}\left[F(S)\theta_0+\frac{\epsilon_g(1+\tau_a S)}{S(1+\tau_a S)+K_1L}+\frac{\epsilon_p(S)(1+\tau_g S)(1+\tau_a S)}{h(S(1+\tau_a S)+K_1L)}+\frac{K_1L\epsilon_a}{S(1+\tau_a S)+K_1L}\right]$$

Figure 29.- Schematic of servo-levelled platform using gyroscope and accelerometer control -- No passive isolation

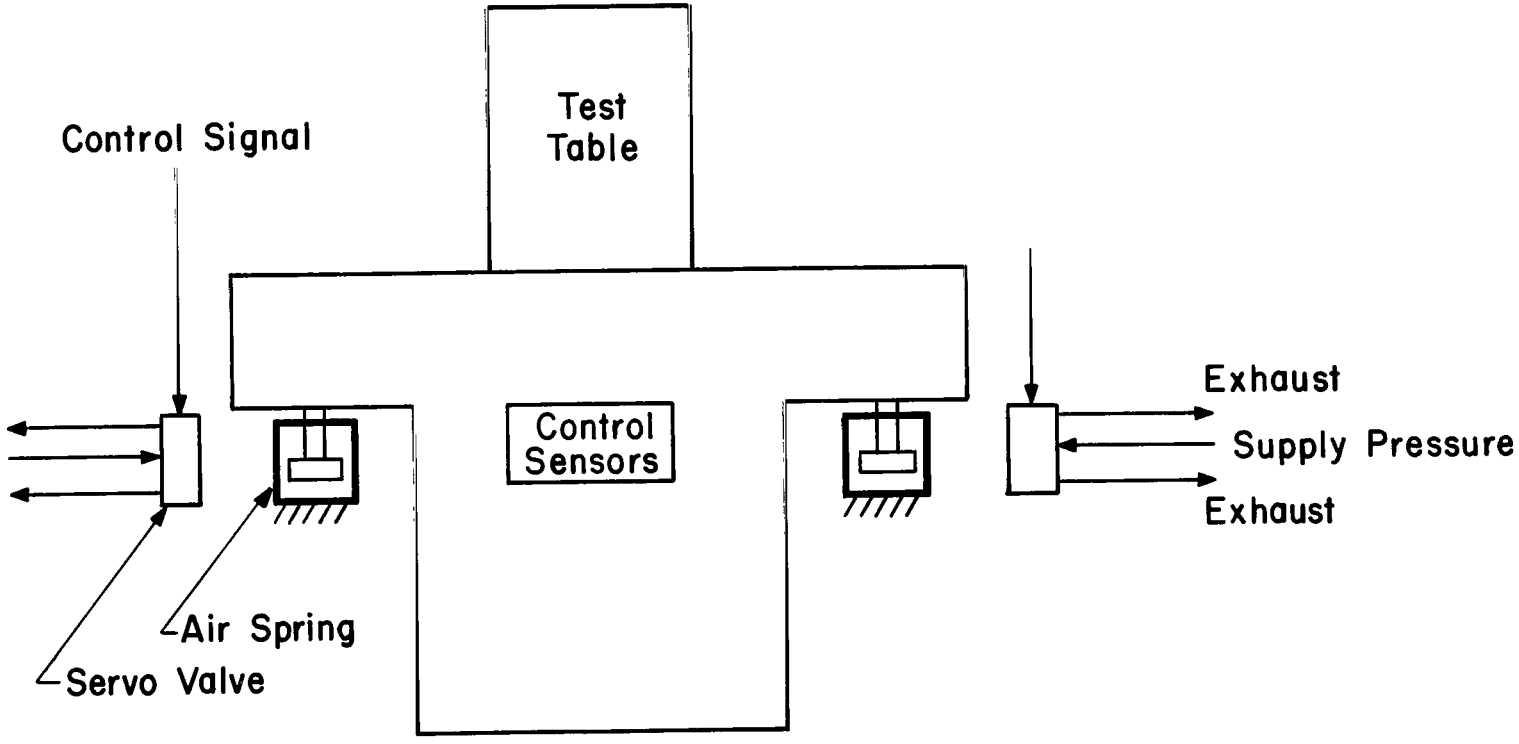

Figure 30.- Schematic of servo-levelled platform using inertial sensors for control and passive high-frequency isolation

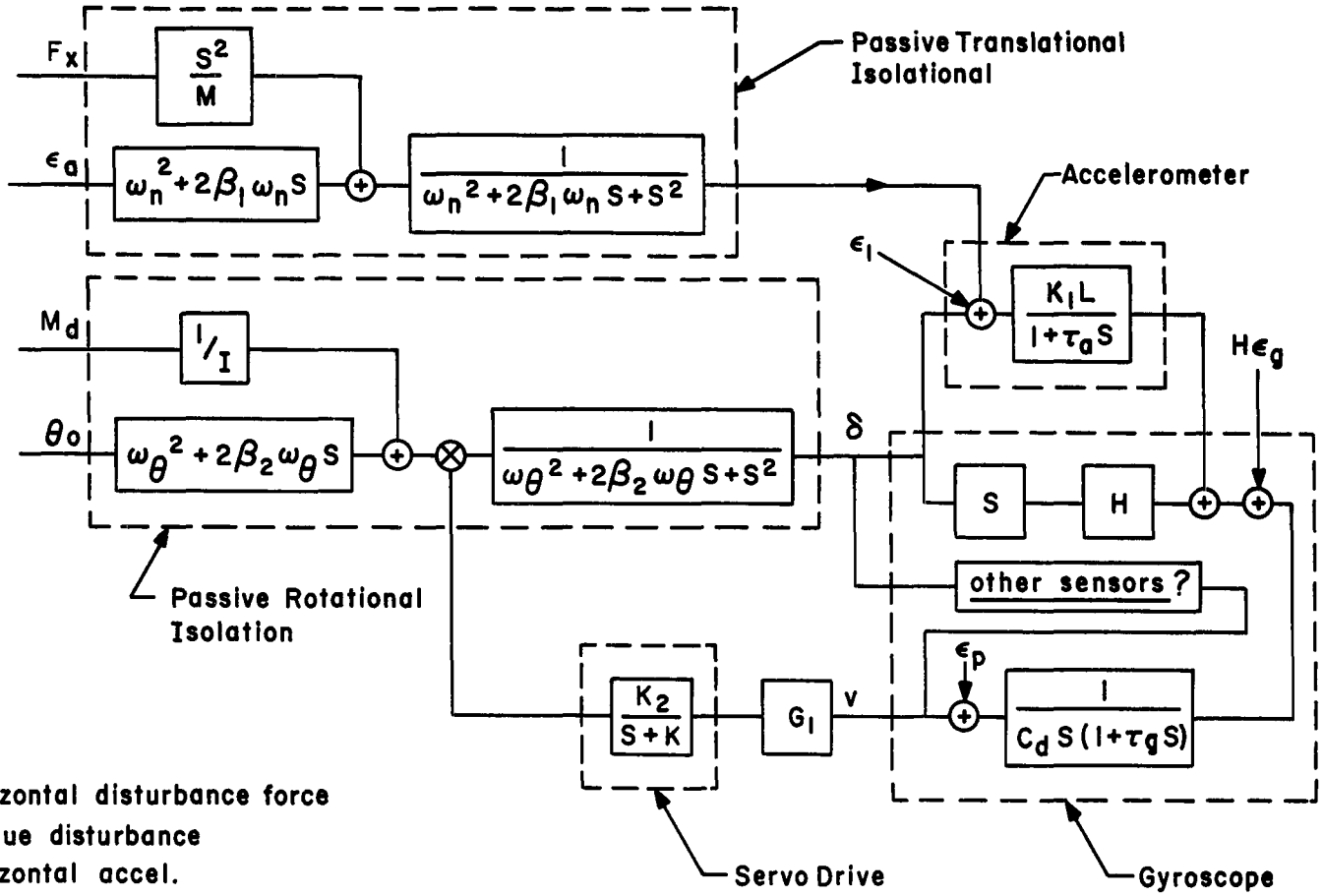

Figure 31.- Schematic of active isolation system using gyroscope and accelerometer control with passive isolation

angle δ will be determined. After the control sensors are selected, various configurations and drives will be investigated for the design of the best platform.

Accelerometer Test Station

As discussed in Section III, the major problem in bias measurement of accelerometers is angular motions relative to gravity. It is, therefore, expected that the gyroscope test station design, with some modifications, will be suited for accelerometer bias measurement as well. Design considerations for threshold measurement will be deferred until the gyroscope test station design is completed.

Electronics Research Center
National Aeronautics and Space Administration
Cambridge, Massachusetts, August 26, 1966
125-17-01-01-80

REFERENCES

1. Weiher, T. E. : Progress in Test Pad Stability. AIAA/ION, Guidance and Control Conference, Minneapolis, Minn., August 16-18, 1965.

2. Mathis, L. O., Stephens, J. R., and Wright, S. C. : The Design and Construction of an Inertial Test Facility. A1AA/ION, Guidance and Control Conference, Minneapolis, Minn., August 16-18, 1965.

3. McNeill, R. L., Margason, B. E., and Babcock, F. M. : The Role of Soil Dynamics in the Design of Stable Test Pads. AIAA/ION, Guidance and Control Conference, Minneapolis, Minn., August 16-18, 1965.

4. Weinstock, H. : Specification for the Permissible Motions of a Platform for Performance Evaluation of the Single Degree of Freedom Integrating Gyroscope. MIT Instrumentation Laboratory, Report No. E-1267, December 1962.

5. Wardin, R., and Werner, W. : Test Pad Requirements for Free Gyros. Honeywell Aeronautical Division, Minneapolis, Minn., February 1964.

6. Preskitt, S. V., and Fix, J. E. : Six Degree of Freedom Test Podium at the United States Air Force Standards Calibration Laboratory. Technical Report No. 63-46, The Geotechnical Corporation, Garland, Texas, May 1963.

7. Tsutsumi, K. : A Ground Tilt Isolation Platform. Report No. E-1508, M. I. T. Instrumentation Laboratory, January 1964.

8. Cooper, Lt. John R. : A Statistical Analysis of Gyro Drift Test Data. M. I. T. Experimental Astronomy Laboratory, Report No. TE-13, S. M. Thesis, Department of Aeronautics and Astronautics, M. I. T., September 1965.

9. Weinstock, H. : Statistical Analysis of Sixteen Earth Reference Drift Tests on 4FBG Gyroscopes. Report No. E-1486, M. I. T. Instrumentation Laboratory, April 1964.

10. Marshall, R. E., and Palmer, P. J. : Inertial Instrument Design Verification Tests for High-G Applications. Report No. E-1866, M. I. T. Instrumentation Laboratory, October 1965.

11. Lerwick, T. R. : Power Spectral Analysis of GG159C1#5 Gyro Drift Rate. Memorandum to C. A. Edstrom, Honeywell Aeronautical Division, Minneapolis, Minn., May 16, 1963.

12. Buchanan, J. M. : Test Methods and Performance Parameters for Inertial Navigation Equipment. Report No. R-413, M. I. T. Instrumentation Laboratory, June 1963.

13. Palmer, P. J. : Gyro Torque Coefficients. Report No. E-1601, M. I. T. Instrumentation Laboratory, March 1965.

14. Denhard, W. G. : Laboratory Testing of a Floated Single Degree of Freedom Integrating Inertial Gyro. Report No. R-105, M. I. T. Instrumentation Laboratory, September 1956.

15. Cannon, R. H. : Kinematic Drift of Single Axis Gyroscopes. Journal of Applied Mechanics, June 1958.

16. Goodman, L. E. , and Robinson, A. R. : Effect of Finite Rotations of Gyroscope Sensing Devices. Journal of Applied Mechanics, June 1958.

17. Weinstock, H. , and Marchese, V. : Frequency Response Characteristics of a Typical Single Degree of Freedom Integrating Gyroscope. Report No. E-1721, M. I. T. Instrumentation Laboratory, January 1965.

18. Weinstock, H. : Effects of Angular Vibration on Gyroscope Instruments. Session 11 of notes from Summer 1963 Program 16. 39S, Inertial Navigation Equipment Evaluation Techniques, M. I. T. , August 1963.

19. Hildebrand, F. B. : Methods of Applied Mathematics. Prentice Hall, Inc. , Englewood Cliffs, N. J. 1952.

20. Housner, G. W. : Vibration of Structures Induced by Seismic Waves. Section 50 of Shock and Vibration Handbook, C. M. Harris and C. E. Crede, Editors, McGraw Hill Book Company, New York, 1961.

21. Problems in Seismic Background Noise. Acoustics and Seismics Laboratory, Institute of Science and Technology, University of Michigan, Ann Arbor, Michigan.

22. Frantti, G. E. : Investigation of Short Period Seismic Noise in Major Physiographic Environments of Continental United States. University of Michigan, Prepared for Air Force Cambridge Research Laboratories, Report No. AFCRL 65-406, June 1965.

23. Iyer, H. M. : The History and Science of Microseisms. Acoustics and Seismics Laboratory, University of Michigan, April 1964.

24. Brune, J. N. , and Oliver, J. : The Seismic Noise of the Earth's Surface. Bulletin of Seismological Society of America, vol. 49, No. 4, October 1959.

25. Haubrich, R. A. , and MacKenzie, G. S. : Earth Noise, 5-500 Millicycles per Second. Journal of Geophysics Research, vol. 70, 1965.

26. Kamperman, G. W. : Vibration Isolation Effectiveness of Inertia Pads Resting on Soil. Journal of Spacecraft, March-April, 1965.

27. Mihm, J. : Seismic Study of Kendall Square, Preliminary Report No. 1. Report No. ERC-PM-66-1, NASA, Electronics Research Center, January 1966.

28. Smith, S. W. : Free Oscillations Excited by The Alaskan Earthquake. Journal of Geophysics Research, vol. 71, No. 4, February 1966.

29. Jeffreys, H. : The Earth. Cambridge University Press, Cambridge, England, Third Edition, 1952.

30. Gamow, G. : A Planet Called Earth. Viking Press, New York, 1963.

31. Oliver, J. : Long Earthquake Waves. Scientific American, March 1959.

APPENDIX

SUPPLEMENTARY DEFINITION OF SYMBOLS

Arabic Letter Symbols :

In the interest of brevity and continuity, several symbols in the body of this report have not been defined in text where their definitions could be inferred by readers well versed in inertial navigation sensor and system design. The following list defines additional symbols which supplement the definitions provided in the report body.

a = Acceleration along sensitive axis of the instrument

a_X = Horizontal component of ground acceleration

a_Z = Vertical component of ground acceleration

$A(S)$ = Accelerometer performance function

$A_{(C-F)OA}$ = Angular displacement of gimbal (float) of a single-degree-of-freedom gyroscope about the output axis as measured from the case of the instrument

$A_{(I-C)IA}$ = Angular displacement of the case of a single-degree-of-freedom gyroscope about the sensitive (input) axis of the instrument measured from an inertial reference frame

$A_{(I-C)OA}$ = Angular displacement of the case of a single-degree-of-freedom gyroscope about the output axis measured from an inertial reference frame

$A_{(I-C)SRA}$ = Angular displacement of the case of a gyroscope about a case-fixed axis corresponding to the direction of the rotor angular momentum when instrument is at null

$A_{(I-C)SRA^*}$ = Angular displacement of a gyroscope instrument about a space-fixed axis corresponding to the direction of the rotor angular momentum when instrument is both at rest and at null

$A_{(I-F)OA}$ = Angular displacement of gimbal (float) of a single-degree-of-freedom-gyroscope measured from an inertial reference frame

B_g = Gyroscope damping constant

B_p = Platform damping constant

C = Effective damping constant

C_d = Damping constant

C_p = Effective platform and drive damping constant

D = Scale factor for gyroscope drift compensation loop

f - Frequency of motion

f = Friction torque

g = Equivalent acceleration of gravity

G(S) = Characteristic function of compensation network

H = Gyroscope angular momentum

I = Effective moment of inertia

I_o, I_p = Platform moment of inertia

I_g = Gyroscope gimbal moment of inertia

I_{FOA} = Moment of inertia of gimbal (float) of single-degree-of-freedom gyroscope (excluding rotor) about the output axis of the instrument

I_w = Moment of inertia of gyroscope rotor about a radial axis

IA = Sensitive (input) axis of the gyroscope rotor of a single-degree-of-freedom gyroscope

IRA = Input reference axis-- case-fixed axis corresponding to input axis (IA) when instrument is at null

$j = \sqrt{-1}$

$j\omega$ = Complex frequency variable

K_p = Platform pendulosity

K_g = Gyroscope elastic restraint (stiffness)

K(S) = Torque motor sensitivity and loop compensation characteristics.

K_i = Scale factor or gain

L_i = Characteristic function of compensation network

M = Platform mass

M_d = Disturbing torques

ml = Pendulousity of pendulum instrument (gram-cm or equivalent units)

R = Accelerometer sensitivity to rotational acceleration

S = Laplace transform variable

SA = Direction of gyroscope rotor angular momentum

SRA = Spin reference axis of single-degree-of-freedom gyroscope fixed to instrument case and coinciding with angular momemtum vector when instrument is at null

SRA* = Space-fixed axis that corresponds to spin reference axis when there is no angular displacement of the instrument

T_d = Disturbance torques

T_e = Error torques

T_m = Torque applied by torque motor

v = Velocity of vibratory wave

v = Weighted error signal

W = Platform weight

x = Position coordinate

z = Vertical ground displacement

z_o = Amplitude of vertical ground displacement

Greek Letter Symbols :

β = Ratio of damping to critical damping for second-order systems

β_1 = Damping ratio of passive isolation system in translation

β_2 = Rotational damping ratio of passive isolation system

δ = Angle between platform normal and true vertical

ε_a = Disturbance signal caused by horizontal acceleration

ε_g = Gyroscope drift rate

ε_p = Gyroscope pickoff noise

θ = Angle between instrument case and pendulum

θ_o = Angle between normal to Earth surface and "true" vertical

θ_s = Angle between normal to Earth surface and "true" vertical

θ_g = Gyroscope gimbal angle

θ_{pg} = Gyroscope pickoff noise

θ_o = Angular displacement of pendulum base

τ = Time constant

τ_1 = Transducer time constant

τ_a = Accelerometer time constant

τ_g = Gyroscope characteristic time

ϕ = Angle between platform level and Earth surface normal

$\Phi_{aa}(f)$ = Linear acceleration power spectral density $(g\text{-peak})^2/cps$

$\Phi_{ee}(f)$ = Angular vibration power spectral density $(arc\text{-}sec\ peak)^2/cps$

$\omega = 2\pi f$ = circular frequency of applied motion

ω_a = Characteristic circular frequency of system performance equation

ω_n = Natural circular frequency of second-order system.

"The aeronautical and space activities of the United States shall be conducted so as to contribute . . . to the expansion of human knowledge of phenomena in the atmosphere and space. The Administration shall provide for the widest practicable and appropriate dissemination of information concerning its activities and the results thereof."

—NATIONAL AERONAUTICS AND SPACE ACT OF 1958

NASA SCIENTIFIC AND TECHNICAL PUBLICATIONS

TECHNICAL REPORTS: Scientific and technical information considered important, complete, and a lasting contribution to existing knowledge.

TECHNICAL NOTES: Information less broad in scope but nevertheless of importance as a contribution to existing knowledge.

TECHNICAL MEMORANDUMS: Information receiving limited distribution because of preliminary data, security classification, or other reasons.

CONTRACTOR REPORTS: Technical information generated in connection with a NASA contract or grant and released under NASA auspices.

TECHNICAL TRANSLATIONS: Information published in a foreign language considered to merit NASA distribution in English.

TECHNICAL REPRINTS: Information derived from NASA activities and initially published in the form of journal articles.

SPECIAL PUBLICATIONS: Information derived from or of value to NASA activities but not necessarily reporting the results of individual NASA-programmed scientific efforts. Publications include conference proceedings, monographs, data compilations, handbooks, sourcebooks, and special bibliographies.

Details on the availability of these publications may be obtained from:

SCIENTIFIC AND TECHNICAL INFORMATION DIVISION

NATIONAL AERONAUTICS AND SPACE ADMINISTRATION

Washington, D.C. 20546